

1 **Mass balance of the ice sheets and glaciers – progress since AR5 and challenges**

2 **EARTH SCIENCE REVIEWS invited review/synthesis paper**

3 **30 September 2019 revised version**

4
5 Edward Hanna¹, Frank Pattyn², Francisco Navarro³, Vincent Favier⁴, Heiko Goelzer^{2,5},
6 Michiel R. van den Broeke⁵, Miren Vizcaino⁶, Pippa L. Whitehouse⁷, Catherine Ritz⁴, Kevin
7 Bulthuis^{8,2}, Ben Smith⁹

8

9 ¹School of Geography and Lincoln Centre for Water and Planetary Health, University of
10 Lincoln, Lincoln, UK, ehanna@lincoln.ac.uk

11 ²Laboratoire de Glaciologie, Université Libre de Bruxelles, Brussels, Belgium

12 ³Departamento de Matemática Aplicada a las Tecnologías de la Información y las
13 Comunicaciones, Universidad Politécnica de Madrid, Madrid, Spain

14 ⁴CNRS, Univ. Grenoble Alpes, Institut des Géosciences de l'Environnement (IGE), 38000
15 Grenoble, France

16 ⁵Institute for Marine and Atmospheric Research, Utrecht University, Utrecht, The
17 Netherlands

18 ⁶Department of Geoscience and Remote Sensing, Delft University of Technology, Delft, The
19 Netherlands

20 ⁷Department of Geography, University of Durham, Durham, UK

21 ⁸Computational and Stochastic Modeling, Aerospace and Mechanical Engineering, Université
22 de Liège, Liège, Belgium

23 ⁹Polar Science Center, Applied Physics Lab, University of Washington, Seattle, USA

24
25
26
27 **Abstract.** Recent research shows increasing decadal ice mass losses from the Greenland and
28 Antarctic Ice Sheets and more generally from glaciers worldwide in the light of continued
29 global warming. Here, in an update of our previous ISMASS paper (Hanna et al., 2013), we
30 review recent observational estimates of ice sheet and glacier mass balance, and their related
31 uncertainties, first briefly considering relevant monitoring methods. Focusing on the response
32 to climate change during 1992-2018, and especially the post-IPCC AR5 period, we discuss
33 recent changes in the relative contributions of ice sheets and glaciers to sea-level change. We
34 assess recent advances in understanding of the relative importance of surface mass balance
35 and ice dynamics in overall ice-sheet mass change. We also consider recent improvements in
36 ice-sheet modelling, highlighting data-model linkages and the use of updated observational
37 datasets in ice-sheet models. Finally, by identifying key deficiencies in the observations and
38 models that hamper current understanding and limit reliability of future ice-sheet projections,
39 we make recommendations to the research community for reducing these knowledge gaps.
40 Our synthesis aims to provide a critical and timely review of the current state of the science
41 in advance of the next Intergovernmental Panel on Climate Change Assessment Report that is
42 due in 2021.

1.0 Introduction

Major uncertainties in predicting and projecting future sea-level rise are due to the contribution of the two major ice sheets on Earth, Greenland and Antarctica (Pattyn et al., 2018). These uncertainties essentially stem from the fact that both ice sheets may reach a tipping point, in this context defined as (regionally) irreversible mass loss, with a warming climate and that the timing of the onset of such a tipping point is difficult to assess. This is particularly true for the Antarctic Ice Sheets (AIS), where two instability mechanisms potentially operate, allowing a large divergence in timing of onset and mass loss in model projections, while the Greenland Ice Sheet (GrIS) is also particularly susceptible to increased mass loss from surface melting and associated feedbacks under anthropogenic warming.

The Expert Group on Ice Sheet Mass Balance and Sea Level (ISMAS; <http://www.climate-cryosphere.org/activities/groups/ismass>) convened a one-day workshop as part of POLAR2018 in Davos, Switzerland, on 15 June 2018, to discuss advances in ice-sheet observations and modelling since the Fifth Assessment Report of the Intergovernmental Panel on Climate Change (IPCC AR5). The talks and discussions are summarised here in an update of our previous review (Hanna et al., 2013) where we synthesised material from a similar workshop held in Portland, Oregon, USA, in July 2012. Here we focus, in the light of advances in the last six years, on what we need to know in order to make improved model projections of ice-sheet change. Apart from providing an update of recent observational estimates of ice-sheet mass changes, we also set this in a wider context of global glacier change. The paper is arranged as follows. In section (2) we discuss recent advances in ice-sheet observations, while section (3) focuses on advances in modelling and identifies remaining challenges – including links with observational needs - that need to be overcome in order to make better projections. Section (4) discusses recent and projected mass-balance rates for glaciers and ice caps, comparing these with recent ice-sheet changes, setting the latter in a broader context of global glacier change. Finally, in section (5) we summarise our findings and make key recommendations for stimulating further research.

2.0 Observational estimates of ice-sheet total and surface mass balance

In this section we summarise recent observation-based estimates of the total mass balance of the Antarctic and Greenland ice sheets, also considering changes in surface mass balance (SMB; net snow accumulation minus surface meltwater runoff) and – for marine-terminating glaciers – ice dynamics (solid ice dynamical discharge across the grounding line – the contact of an ice sheet with the ocean where the ice mass becomes buoyant and floats – and subsequent calving of icebergs) where appropriate (**Figure 1**). **Figure 2** shows mean SMB for the ice sheets for recent periods, while mean surface ice flow velocity maps can be found in Rignot et al. (2019) and Mouginot et al. (2019) (Fig. 1A in both papers). Satellite, airborne and in situ observational techniques and modelling studies have provided a detailed representation of recent ice-sheet mass loss and increases in ice melt and discharge (Moon et al., 2012; Enderlin et al., 2014; Bigg et al., 2014; Shepherd et al., 2012, 2018; Trusel et al. 2018; Rignot et al., 2019; Mouginot et al., 2019).

There are three main methods of estimating ice-sheet mass changes. Firstly, radar and laser altimetry (mainly using CryoSat, Envisat, ERA and ICESat satellites), which measure changes in height of the surface over repeat surveys that are interpolated over the surface area of interest to estimate a volume change which is converted into a mass change. This latter is typically done using knowledge or assumptions of the radar return depth and/or near-surface density. Alternatively Zwally et al. (2015) use knowledge of the accumulation-driven mass anomaly during the period of observation, together with the associated accumulation-driven

101 elevation anomaly corrected for the accumulation-driven firn compaction, to derive the total
102 mass change and its accumulation- and dynamic-driven components Secondly, satellite
103 gravimetry effectively weighs the ice sheets through their gravitational pull on a pair of
104 orbiting satellites called GRACE (or, since May 2018, the subsequent GRACE Follow On
105 mission). Thirdly, the mass budget or component method compares SMB model output with
106 multi-sensor satellite radar observations of ice velocity across a position on or close to the
107 grounding line, from which ice discharge can be inferred if the thickness and vertical velocity
108 profile of ice at that point are also assumed/known. All three methods have their strengths and
109 weaknesses (e.g. Hanna et al., 2013; Bamber et al., 2018). Altimetry and, especially,
110 gravimetry, require accurate quantification of Glacial Isostatic Adjustment (GIA; Section 2.3)
111 which contaminates the ice-sheet mass loss signals. Gravimetry is limited by a relatively
112 short time series (since 2002) and low spatial resolution (~300 km) compared with the other
113 methods but is the method that most directly measures mass change.

114 Altimetry surveys, which date relatively far back to the early 1990s, provide elevation
115 changes that need to be converted into volume and then mass changes, requiring knowledge
116 of near-surface density which is often highly variable and uncertain for ice sheets. In
117 addition, radar altimeter surveys do not adequately sample relatively steeper-sloping ice-sheet
118 margins and require correction for the highly-variable radar-reflection depth that has strong
119 seasonal variations and interannual trends and complex interactions between linearly-
120 polarized radar signals and the direction of the surface slope. Successful corrections have
121 been developed and applied to radar altimeter data from ERS1 and ERS2 using crossover
122 analysis data (Wingham et al., 1998; Davis and Ferguson, 2004; Zwally et al., 2005; Yi et al.,
123 2011; Khvorostovsky, 2012) and to Envisat data using repeat track analysis and an advanced
124 correction algorithm (Filament and Remy, 2012). However, the corrections applied by others
125 to Envisat and CryoSat data have been questioned due to complex interaction of the cross-
126 track linearly-polarized radar signal of Envisat and CryoSat with the surface slope that affects
127 the highly-variable penetration/reflection depth (Zwally et al., 2016; Nilsson et al., 2016).
128 Also, allowance must be made for firn-compaction changes arising from temperature and/or
129 accumulation variations, especially in the context of a warming ice-sheet, which significantly
130 affect surface elevation without mass change (e.g. Li and Zwally, 2015; Zwally et al., 2015).
131 A number of the altimetry studies included here have used a regionally-varying, temporally
132 constant effective density value to convert observed volume changes to mass change
133 estimates. In many cases, a low effective density is assigned for inland areas, and a high
134 effective density in coastal errors. Because in Greenland and much of Antarctica, coastal
135 areas are thinning while inland areas are in neutral balance or thickening, this can produce
136 negative biases in estimated ice-sheet mass-change rates if the changes in the interior are
137 associated with long-term imbalance between ice flow and snow accumulation.

138 The mass-budget method involves subtracting two large quantities (SMB and
139 discharge) and needs detailed and complete regional information on these components, which
140 is recently available from satellite radar data for discharge. SMB cannot be directly measured
141 at the ice-sheet scale but is instead estimated using regional climate models that are evaluated
142 and calibrated using in-situ climate and SMB observations. These RCM/SMB models can
143 have significant uncertainties in derived accumulation and runoff (of the order of 15%, e.g.
144 Fettweis, 2018). Deriving discharge requires knowledge of bathymetry and the assumption of
145 an internal velocity profile in order to determine ice flux across the grounding line, and there
146 are also errors in determining the position of the grounding line. Further uncertainty arises in
147 estimating the discharge from the areas where the ice velocity is not measured. Despite these
148 significant uncertainties, an advantage of this method is that the mass change can be
149 partitioned into its (sub-)components.

150

151 A more recent group use combinations of measurement strategies to minimize the
152 disadvantages of each, such as by combining altimetric with gravimetric data (Sasgen et al,
153 2019) or mass-budget data with gravimetric data (e.g. Talpe et al, 2017) to simultaneously
154 estimate GIA rates and ice-sheet mass-balance rates. These studies typically report errors
155 comparable to those reported by single-technique studies, but their results may be seen as
156 more credible because they provide self-consistent solutions for the most important error
157 sources affecting other studies.

158 A major international research programme called the Ice-sheet Mass Balance Inter-
159 comparison Exercise (IMBIE; <http://imbie.org/>) has attempted to reconcile differences
160 between these various methods, and its second phase IMBIE2 has recently reported an
161 updated set of reconciled total mass balance estimates for Antarctica (Shepherd et al., 2018)
162 and is shortly expected to update previous results for Greenland. However, despite recent
163 improvements in coverage and accuracy, modern satellite-based records are too short for
164 attribution studies aiming to separate the contributions from anthropogenic greenhouse gas
165 warming signal and background climate variability to the contemporary mass loss (Wouters
166 et al., 2013), and proxy data such as ice cores are therefore used to overcome this limitation.

167 We have compiled recent estimates of mass balance using available (at the time of
168 writing) published references from 2014 to 2019 (**Figure 3**), in an update of Figure 1 in
169 Hanna et al. (2013). Our new box plots clearly show continuing significant mass losses from
170 both ice sheets, with approximately double the recent rate of mass loss for Greenland
171 compared with Antarctica. However, the boxes tend to suppress the considerable interannual
172 variability of mass fluctuations, e.g. the record loss of mass from the GrIS in 2012, and this
173 shorter-term variability is strikingly shown by annually-resolved time series based on the
174 mass-budget method [Figure 3 of Rignot et al. (2019) for Antarctica and Figure 3 of
175 Mougnot et al. (2019) for GrIS].

176

177 *2.1 Antarctic ice sheets*

178

179 Recent work agrees on significant and steadily growing mass losses from the West Antarctic
180 Ice Sheet (WAIS) and the Antarctic Peninsula but highlights considerable residual
181 uncertainty regarding the recent contribution of the East Antarctic Ice Sheet (EAIS) to global
182 sea-level rise (SLR) (Shepherd et al., 2018; Rignot et al., 2019). For Antarctica there is
183 relatively little surface melt and subsequent runoff, and surface accumulation has been
184 relatively stable, although recent reports show an increase in AIS snowfall (Medley and
185 Thomas, 2019). In Antarctica, the main sustained mass losses are through ice dynamics,
186 expressed as increased ice discharge across the grounding line. Mass loss through this
187 mechanism occurs primarily through increased flow speeds of marine terminating glaciers in
188 the Amundsen and Bellingshausen Sea sectors, which are sensitive to ocean warming,
189 although superimposed on these relatively gradual changes there are significant short-term,
190 i.e. interannual to decadal, SMB variations (Rignot et al., 2019). As a key output of the
191 IMBIE2 project, Shepherd et al. (2018) built on Shepherd et al. (2012) by significantly
192 extending the study period and reconciling the results of 24 independent estimates of
193 Antarctic ice-sheet mass balance using satellite altimetry, gravimetry and the mass budget
194 methods encompassing thirteen satellite missions and approximately double the number of
195 studies previously considered. They found that between 1992-2017 the Antarctic ice sheets
196 lost 2725 ± 1400 Gt of ice, therefore contributing 7.6 ± 3.9 mm to SLR, principally due to
197 increased mass loss from the WAIS and the Antarctic Peninsula. However, they also found
198 that EAIS was close to balance, i.e. 5 ± 46 Gt yr⁻¹ averaged over the 25 years, although this
199 was the least certain region, attributed to its enormous area and relatively poorly constrained
200 GIA (Section 2.3) compared with other regions. Shepherd et al. (2018) found that WAIS

201 mass loss steadily increased from 53 ± 29 Gt yr⁻¹ for 1992-1996 to 159 ± 26 Gt yr⁻¹ during
202 2013-2017, and that Antarctic Peninsula mass losses increased by 15 Gt yr⁻¹ since 2000,
203 while the EAIS had little overall trend in mass balance during the period of study. The overall
204 reconciled sea-level contribution from Antarctica rose correspondingly from 0.2 to 0.6 mm
205 yr⁻¹. These authors also reported no systematic Antarctic SMB trend, and they therefore
206 attributed WAIS mass loss to increased ice discharge. Of particular concern is the case of
207 ongoing grounding line retreat in the Amundsen Sea in West Antarctica, as well as basal melt
208 of ice shelves through polynya-related feedbacks, e.g. in the Ross Sea (Stewart et al., 2019).

209 Rignot et al. (2019) used the mass budget method to compare Antarctic snow
210 accumulation with ice discharge for 1979-2017, using improved, high-resolution datasets of
211 ice-sheet velocity and thickness, topography and drainage basins and modelled SMB. Within
212 uncertainties their total mass balance estimates for WAIS and the Antarctic Peninsula agreed
213 with those of Shepherd et al. (2018) but they derived a -57 ± 2 Gt yr⁻¹ mass balance for East
214 Antarctica for 1992-2017, compared with the $+5\pm 46$ Gt yr⁻¹ for the same period derived in
215 IMBIE2. Possible reasons for this difference include uncertainties in ice thickness and
216 modelled SMB in the mass budget method, together with further uncertainties in the IMBIE-
217 2 EAIS mass estimates arising from volume to mass conversions within the altimetry data
218 processing and significantly uncertain GIA corrections when processing GRACE data.
219 Zwally et al. (2015) found significant EAIS mass gains of 136 ± 50 Gt yr⁻¹ for 1992-2001
220 from ERS radar altimetry and 136 ± 28 Gt yr⁻¹ for 2003-2008 based on ERS radar altimetry
221 and ICESat laser altimetry, dynamic thickening of 147 ± 55 Gt yr⁻¹ and 147 ± 34 Gt yr⁻¹
222 respectively, and accumulation-driven losses of 11 ± 6 Gt yr⁻¹ in both periods with respect to
223 a 27-year mean. They attributed the dynamic thickening to a long-term dynamic response
224 arising from a 67-266% increase in snow accumulation during the Holocene, as derived from
225 six ice cores (Siegert, 2003), rather than contemporaneous increases in accumulation.
226 However, because the results of Zwally et al. (2015) differ from most others, they have been
227 questioned by other workers (Scambos and Shuman, 2016; Martín-Español et al., 2017),
228 although see Zwally et al. (2016) for a response. Bamber et al. (2018) describe “reasonable
229 consistency between [EAIS mass balance] estimates” if they discount the outlier of Zwally et
230 al. (2015). Notwithstanding, as highlighted by Hanna et al. (2013) and Shepherd et al. (2018)
231 and clearly shown here in **Figure 3** which clearly shows ‘outliers’ on both sides of the
232 IMBIE-reconciled means, disparate estimates of the mass balance of East Antarctica, which
233 vary by ~ 100 Gt yr⁻¹, have not yet been properly resolved. Furthermore, the range of
234 differences does not appear to be narrowing with time, which indicates a lack of advancement
235 in one or more of the mass-balance determination methods.

236 237 *2.2 Greenland Ice Sheet*

238
239 According to several recent estimates, the GrIS lost 257 ± 15 Gt yr⁻¹ of mass during 2003-
240 2015 (Box et al., 2018), 262 ± 21 Gt yr⁻¹ during 2007-2011 (Andersen et al., 2015), 269 ± 51
241 Gt yr⁻¹ during 2011-2014 (McMillan et al., 2016), 247 Gt yr⁻¹ of mass – representing 37% of
242 the overall land ice contribution to global sea-level rise – during 2012-2016 (Bamber et al.
243 2018), and 286 ± 20 Gt yr⁻¹ during 2010-2018 (Mouginot et al., 2019). A slightly greater mass
244 loss of 308 ± 12 Gt yr⁻¹ based on GRACE gravimetric satellite data for 2007-2016 was given
245 by Zhang et al. (2019). Some of the difference between these numbers can be attributed to
246 different methods considering either just the contiguous ice sheet or also including
247 disconnected peripheral glaciers and ice caps, the latter being the case for GRACE-based
248 estimates. However, GrIS mass loss approximately quadrupled during 2002/3 to 2012/13
249 (Bevis et al., 2019). The GrIS sea-level contribution over 1992-2017 was approximately one

250 and a half times the sea-level contribution of Antarctica (Box et al., 2018). However this kind
251 of average value masks very significant interannual variability of $\pm 228 \text{ Gt yr}^{-1}$, and even 5-
252 year mean values can vary by $\pm 102 \text{ Gt yr}^{-1}$, based on 2003-2016 data; for example recent
253 annual mass losses ranged from $>400 \text{ Gt}$ in 2012 (a record melt year caused by jet-stream
254 changes, e.g. Hanna et al., 2014) to $<100 \text{ Gt}$ just one year later (Bamber et al., 2018).

255 McMillan et al. (2016) found that high interannual (1991-2014) mass balance
256 variability was mainly due to changes in runoff of 102 Gt yr^{-1} (standard deviation, $\sim 28\%$ of
257 the mean annual runoff value) with lesser contributions from year-to-year snowfall variations
258 of $\sim 61 \text{ Gt yr}^{-1}$ ($\sim 9\%$ of the mean snowfall value) and solid ice discharge of $\sim 20 \text{ Gt yr}^{-1}$ ($\sim 5\%$
259 of the mean annual discharge). Their interpretation of transient mass changes was supported
260 by Zhang et al. (2019) who attributed big short-term (~ 3 -year) fluctuations in surface mass
261 balance to changes in atmospheric circulation, specifically the Greenland Blocking Index
262 (GBI; Hanna et al. 2016), with opposite GBI phases in 2010-2012 (highly positive GBI) and
263 2013-2015 (less blocked Greenland). Also, in the MODIS satellite record since the year 2000,
264 Greenland albedo was relatively high from 2013-2018 after reaching a record low in 2012
265 (Tedesco et al., 2018). The relatively low GrIS mass loss in 2013-14 was termed the “pause”
266 (Bevis et al., 2019). However, Zhang et al. (2019) inferred an acceleration of $18 \pm 9 \text{ Gt yr}^{-2}$ in
267 GrIS mass loss over 2007-2016. Given this pronounced recent short-term variability, for
268 example the recent slowdown of rapid mass loss increases in the 2000s and very early 2010s,
269 such trends should only be extrapolated forward with great caution.

270 Greenland mass loss is mainly driven by atmospheric warming, and – based on ice-
271 core-derived melt information and regional model simulations – surface meltwater runoff
272 increased by $\sim 50\%$ since the 1990s, becoming significantly higher than pre-industrial levels
273 and being unprecedented in the last 7000 years (Trusel et al., 2018). Enderlin et al. (2014)
274 found an increasingly important role of runoff on total mass annual losses during their 2000-
275 2012 study period and concluded that SMB changes were the main driver of long-term
276 (decadal or longer) mass loss.

277 However, just five marginal glacier near-termini regions, covering $<1\%$ of the GrIS
278 by area were responsible for 12% of the net ice loss (McMillan et al., 2016), highlighting the
279 potentially important role and sensitivity of ice dynamics; these authors alongside Tedesco et
280 al. (2016) also found an atmospheric warming signal on mass balance in the northernmost
281 reaches of the ice sheet. Taking a longer perspective from 1972-2018, using extended
282 datasets of outlet glacier velocity and ice thickness, improved bathymetric and gravity
283 surveys and newly-available high resolution SMB model output, Mougintot et al. (2019)
284 reported that dynamical losses from the GrIS have continuously increased since 1972,
285 dominating mass changes except for the last 20 years, estimating that over this longer period
286 $66 \pm 8\%$ of the overall mass losses were from dynamics and $34 \pm 8\%$ from SMB. They
287 concluded that dynamics are likely to continue to be important in future decades, apart from
288 the southwest where runoff/SMB changes predominate, and that the northern parts of GrIS –
289 where outlet glaciers could lose their buttressing ice shelves – are likely to be especially
290 sensitive to future climate warming.

291 292 *2.3 Glacial Isostatic Adjustment*

293
294 Processes associated with GIA must be accounted for when quantifying contemporary ice-
295 sheet change (Shepherd et al., 2018) and also when predicting the dynamics of future change
296 (Adhikari et al., 2014; Gomez et al., 2015; Konrad et al., 2015). Specifically, ongoing
297 changes to the height of the land surface and the shape of Earth’s gravitational field, in
298 response to past ice-mass change, will bias gravimetry- and altimeter-based measurements of
299 contemporary ice mass balance and alter the boundary conditions for ice sheet dynamics. Due

300 to density differences between the ice sheet and the solid Earth, the impact of GIA on
301 gravimetry measurements will be 4-5 times greater than the impact on altimetry
302 measurements (Wahr et al., 2000).

303 Numerical models can be used to estimate the geodetic signal associated with GIA
304 (Whitehouse et al., 2012; Ivins et al., 2013; Argus et al., 2014) or it can be inferred via data
305 inversion (Gunter et al., 2014; Martín-Español et al., 2016; Sasgen et al., 2017). Both
306 approaches would benefit from better spatial coverage of GPS observations of land
307 deformation, while the first approach strongly depends on past ice sheet change, for which
308 constraints are severely lacking, particularly across the interior of the Greenland and
309 Antarctic ice sheets. Both approaches also typically rely on the assumption that mantle
310 viscosity beneath the major ice sheets is spatially uniform and high enough that the signal due
311 to past ice-mass change is constant in time. However, recent work has revealed regions in
312 both Greenland and Antarctica where mantle viscosity is much lower than the global average
313 (e.g. Nield et al., 2014; Khan et al., 2016; Barletta et al., 2018; Mordret, 2018). This has two
314 important implications. First, in regions where upper mantle viscosity is less than $\sim 10^{19}$ Pa s
315 the response to recent (decadal to centennial) ice-mass change will dominate the GIA signal,
316 and may not be steady in time. In such regions a time-varying GIA correction, which
317 accounts for both the viscous and elastic response to contemporary ice-mass change, should
318 be applied to gravimetry, altimetry and other geodetic observations. Secondly, since GIA acts
319 to reduce the water depth adjacent to a shrinking marine-based ice sheet, this can act to slow
320 (Gomez et al., 2010) or reverse (Kingslake et al., 2018) the rate of ice loss, with the
321 stabilising effect being stronger in regions with low upper mantle viscosity (Gomez et al.,
322 2015; Konrad et al., 2015). To better understand the behaviour and likely future of marine-
323 based ice masses it will be necessary to quantify the spatially-varying strength of this
324 stabilising effect and account for feedbacks between GIA and ice dynamics within a coupled
325 modelling framework (e.g. Pollard et al., 2017; Gomez et al., 2018; Larour et al., 2019;
326 Whitehouse et al., 2019).

327

328 **3.0 Recent advances and challenges in modelling including links with observational** 329 **needs**

330

331 *3.1 Modelling ice-sheet instabilities*

332

333 The marine ice-sheet instability (MISI; **Figure 4**) hypothesises a possible collapse of West
334 Antarctica as a consequence of global warming. This process, first proposed in the 1970s
335 (Weertman, 1974; Thomas and Bentley, 1978), was recently theoretically confirmed and
336 demonstrated in numerical models (Schoof, 2007; Pattyn et al., 2012). It arises from thinning
337 and eventually flotation of the ice near the grounding line, which moves the latter into deeper
338 water where the ice is thicker. Thicker ice results in increased ice flux, which further thins
339 (and eventually floats) the ice, resulting in further retreat into deeper water (and thicker ice)
340 and so on. This instability is activated when the bedrock deepens toward the interior of the
341 ice sheet, i.e., a retrograde bed slope, as is the case for most of the West Antarctic ice sheet.
342 The possibility that some glaciers, such as Pine Island Glacier and Thwaites Glacier, are
343 already undergoing MISI has been suggested (Rignot et al., 2014; Christianson et al., 2016).
344 Thwaites Glacier is currently in a less-buttressed state, and several simulations using state-of-
345 the-art ice-sheet models indicate continued mass loss and possibly MISI or MISI-like
346 behaviour even under present climatic conditions (Joughin et al., 2014; Nias et al., 2016;
347 Seroussi et al., 2017). However, rapid grounding line retreat due to MISI or MISI-like
348 behaviour remains highly dependent on the subtleties of subglacial topography (Waibel et al.,

349 2018) and feedbacks associated with GIA (section 2.3), limiting the predictive behaviour of
350 the onset of MISI. In other words, geography matters.

351 The marine ice cliff instability (MICI) hypothesises (**Figure 4**) collapse of ice cliffs
352 that become unstable and fail if higher than ~ 90 m above sea level, leading to the rapid
353 retreat of ice sheets during past warm (e.g., Pliocene and last interglacial) periods (Pollard et
354 al., 2015; DeConto and Pollard, 2016). MICI is a process that facilitates and enhances MISI
355 once the ice shelf has completely disappeared but can also act alone, for instance where the
356 bed is not retrograde (which prevents MISI). MICI relies on the assumption of perfect plastic
357 rheology to represent failure. Cliff instability requires an a priori collapse of ice shelves and
358 is facilitated by hydro-fracturing through the increase of water pressure in surface crevasses
359 which deepens the latter (Bassis and Walker, 2012; Nick et al., 2013; Pollard et al., 2015).
360 Whether MICI is necessary to explain Pliocene sea-level high stands has been questioned
361 recently (Edwards et al., 2019).

362 The introduction of MICI in one ice-sheet model (DeConto and Pollard, 2016) has
363 profoundly shaken the modelling community, as the mechanism potentially results in future
364 sea-level rise estimates of almost an order of magnitude larger compared with other studies
365 (Figure 5 and Table 1). While projected contributions of the Antarctic ice sheet to sea-level
366 rise by the end of this century for recent studies hover between 0 and 0.45 m (5%-95%
367 probability range), the MICI model occupies a range of 0.2-1.7 m (Figure 5a). The
368 discrepancy is even more pronounced for 2300, where the MICI results and other model
369 estimates no longer agree within uncertainties. Edwards et al. (2019) discuss in detail the
370 results of DeConto and Pollard (2016), related to cliff collapse but also the sensitivity of the
371 driving climate model that overestimates surface melt compared to other CMIP5 models.
372 MICI is a plausible mechanism and is observed on tidewater and outlet glaciers in Greenland
373 and the Arctic. However, whether and how it applies to very large outlet glaciers of the
374 Antarctic ice sheet will require further scrutiny. Evidence from paleo-shelf breakup in the
375 Ross Sea shows that ice-sheet response may be more complicated, including significant lags
376 in the response of grounding line retreat (Bart et al., 2018). In order to accurately model ice-
377 sheet instabilities, motion of the grounding line must be accurately represented. International
378 model inter-comparisons of marine ice-sheet models (MISMIP; MISMIP3d) greatly
379 improved those models in terms of representing grounding-line migration numerically by
380 conforming them to known analytical solutions (Pattyn et al., 2012, 2013). These numerical
381 experiments demonstrated that in order to resolve grounding-line migration in marine ice-
382 sheet models, a sufficiently high spatial resolution needs to be applied, since membrane
383 stresses need to be resolved across the grounding line to guarantee mechanical coupling. The
384 inherent change in basal friction occurring across the grounding line – zero friction below the
385 ice shelf – requires high spatial resolution (e.g., < 1 km for Pine Island Glacier; Gladstone et
386 al., 2012) for an accurate representation of grounding-line migration. Therefore, a series of
387 ice-sheet models have implemented a spatial grid refinement, mainly for the purpose of
388 accurate data assimilation (Cornford et al., 2015; Gillet-Chaulet et al., 2012; Morlighem et
389 al., 2010), but also for further transient simulations where the adaptive mesh approach
390 enables the finest grid to follow the grounding-line migration (Cornford et al., 2013, 2016).
391 These higher spatial resolutions of the order of hundreds of meters in the vicinity of
392 grounding lines also pose new challenges concerning data management for modelling
393 purposes (Durand et al., 2011).

394 395 *3.2 Model initialisation, uncertainty and inter-comparison*

396
397 Despite major improvements in ice-sheet model sophistication, major uncertainties still
398 remain pertaining to model initialisation as well as the representation of critical processes

399 such as basal sliding and friction, ice rheology, ice damage (such as calving and MICI) and
400 sub-shelf melting. New developments in data assimilation methods led to improved
401 initialisations in which the initial ice-sheet geometry and velocity field are kept as close as
402 possible to observations by optimising other unknown fields, such as basal friction coefficient
403 and ice stiffness (accounting for crevasse weakening and ice anisotropy; Arthern and
404 Hindmarsh, 2006; Arthern and Gudmundsson, 2010; Cornford et al., 2015; MacAyeal, 1992;
405 Morlighem et al., 2010, 2013). Motivated by the increasing ice-sheet imbalance of the
406 Amundsen Sea Embayment glaciers over the last 20 years (Shepherd et al., 2018), and
407 supported by the recent boom in satellite data availability, data-assimilation methods are
408 progressively used to evaluate unknown time-dependent fields such as basal drag by using
409 time-evolving states accounting for the transient nature of observations and model dynamics
410 (Gillet-Chaulet et al., 2016; Goldberg et al., 2013, 2015, 2016).

411 Ensemble model runs equally improve the predictive power of models by translating
412 uncertainty in a probabilistic framework. The use of statistical emulators thereby increases
413 the confidence in sampling parameter space (Bulthuis et al., 2019) and helps to reduce
414 uncertainties in ice dynamical contributions to future sea-level rise (Ritz et al., 2015;
415 Edwards et al., 2019). Probability distributions for Antarctica are usually not Gaussian and
416 have a long tail towards high values, especially for high greenhouse warming scenarios
417 (**Figure 5** and **Table 1**).

418 An important step forward since the Fifth Assessment Report of the IPCC (IPCC,
419 2013) is that process-based projections of sea-level contributions from both ice sheets are
420 now organised under the Ice Sheet Model Intercomparison Project for CMIP6 (ISMIP6) and
421 form an integral part of the CMIP process (Eyring et al., 2016; Nowicki et al., 2016; Goelzer
422 et al., 2018a; Seroussi et al., 2019). ISMIP6 is working towards providing projections of
423 future ice-sheet mass changes for the next Assessment Report of the IPCC (AR6). It has
424 recently finished its first set of experiments focussing on the initial state of the ice sheets as a
425 starting point for future projections (Goelzer et al., 2018a; Seroussi et al., 2019), which has
426 seen an unprecedented return from ice-sheet modelling groups globally. With ISMIP6, the
427 ice-sheet modelling community has engaged to evolve to new standards in availability,
428 accessibility and transparency of ice-sheet model output data (e.g. Goelzer et al., 2018b),
429 facilitating model-model and data-model comparison and analysis.

430 ISMIP6 has strengthened the links between the ice-sheet modelling community and
431 other communities of global and regional climate modellers, ocean modellers and remote
432 sensing and observations of ice, ocean and atmosphere.

433

434 *3.3 Ice sheet model-climate model coupling*

435

436 Fully coupled simulations based on state of the art AOGCMs and ISMs are an emerging field
437 of active research (e.g. Fyke et al., 2014a; Fischer et al., 2014; Vizcaino et al., 2015; Reerink
438 et al., 2016; Fyke et al., 2018). This development will help to improve our understanding of
439 processes and feedbacks due to climate-ice sheet coupling in consistent modelling
440 frameworks. However, coupling is challenging due to differences in resolution between
441 climate and ice-sheet models, the computational expense of global climate models, and the
442 need for advanced snow/firn schemes, etc. (a review of these challenges and recent advances
443 is given by Vizcaino, 2014). ISMIP6 is also leading and supporting current coupled
444 modelling efforts (Nowicki et al., 2016).

445 Coupling approaches between atmosphere/ice/ocean/sea ice for the Antarctic ice sheet
446 have been considerably developed since the AR5 (Asay-Davis et al., 2017; Pattyn et al.,
447 2017; Favier et al., 2017; Donat-Magnin et al., 2017) but there is still an important need to
448 document the processes occurring at the interface between ocean and ice. Due to the

449 computational cost, these are limited to a single basin (Seroussi et al., 2017) or intermediate
450 coupling for the whole ice sheet (Golledge et al., 2019). Observations are currently being
451 developed to study the ocean characteristics below the ice shelves using autonomous
452 underwater vehicle (AUVs) or remotely operated vehicle (ROVs) (Jenkins et al., 2010;
453 Kimura et al., 2016; Nicholls et al., 2006) and should offer critical information for modellers.

454 For the Greenland ice sheet, coupled models have been applied to investigate several
455 outstanding questions regarding ice-climate interaction, particularly on multi-century and
456 multi-millennia timescales. Some examples of the topics already addressed include the
457 impacts of meltwater on ocean circulation (Golledge et al., 2019), regional impact of ice-
458 sheet area change (Vizcaino et al., 2008, 2010), effect of albedo and cloud change on future
459 SMB (Vizcaino et al., 2014), and elevation-SMB feedback (Vizcaino et al., 2015). Ongoing
460 work aims to include more interaction processes, such as the effects of ocean warming on ice-
461 sheet stability (Straneo et al., 2013).

462 Due to their high computational cost, simulation ensembles (for ice-sheet parameters
463 as well as climate forcing) are rare in coupled modelling. These ensembles are essential tools
464 for the attribution of on-going mass loss and to constrain uncertainty in century projections.
465 Vizcaino et al. (2015) compared 1850-2300 Greenland ice-sheet evolution with a coupled
466 model forced with three different Representative Concentration Pathways (RCP2.6, RCP4.5
467 and RCP8.5). For the historical and RCP8.5 scenarios, they performed a small ensemble (size
468 three). They found a relatively high uncertainty from climate variability in the simulation of
469 contemporary mass loss. However, this uncertainty was relatively small for the projections as
470 compared with the uncertainty from greenhouse gas scenario.

471
472 *3.4 Earth system/regional climate modelling and surface mass balance modelling: advances*
473 *and challenges*

474 475 3.4.1 General

476
477 The accuracy of SMB model output naturally depends on observations that are available to
478 evaluate the models. Recent efforts to collect, synthesise and quality-control in-situ
479 observations of SMB over the AIS and GrIS have greatly improved our confidence in these
480 measurements (Favier et al., 2013; Machguth et al., 2016; Montgomery et al., 2018), yet the
481 observational density remains too low to estimate ice-sheet wide SMB based on interpolation
482 of these data alone. Uncertainties remain especially large along the ice-sheet margins, where
483 SMB gradients are steepest and data density lowest because of adverse climate conditions
484 (Arthern et al., 2006; Bales et al., 2009). Moreover, most in-situ observations constitute an
485 integrated measurement, providing little insight in SMB component partitioning and seasonal
486 evolution. Suitable co-located meteorological observations enable time-dependent estimates
487 of SMB and surface energy balance components such as snow accumulation, sublimation and
488 melt (van den Broeke et al., 2004, 2011), but especially on the AIS surprisingly few
489 (automatic) weather stations collect sufficient data to do so. In the GrIS ablation zone, the
490 PROMICE automatic weather station (AWS) network has recently resolved this problem
491 (Citterio et al., 2015).

492 Although their performance in simulating ice-sheet SMB is continually improving
493 (Cullather et al., 2014; Vizcaino et al., 2014; Lenaerts et al., 2016; van Kampenhout et al.,
494 2017), Earth System Models (ESMs) currently have insufficient (50-100 km) horizontal
495 resolution in the atmosphere to properly resolve marginal SMB gradients, although
496 downscaling via elevation classes (Lipscomb et al., 2013; Alexander et al., 2019; Sellevold et
497 al., submitted), and upcoming variable-resolution ESMs may alleviate this. Moreover, as they
498 do not assimilate observations, ESMs do not simulate realistic weather. Atmospheric

499 reanalyses have similar low resolution, although this is improved in the recently released
500 ERA5 reanalysis, but do assimilate meteorological observations, and hence can be used to
501 force regional climate models (RCMs) at their boundaries. As a result, RCMs provide
502 reasonably realistic ice-sheet weather at acceptable resolutions: typically 25 km for the full
503 AIS (van Wessem et al., 2018; Agosta et al., 2019) and 5 km for AIS sub-regions (van
504 Wessem et al., 2015; Lenaerts et al., 2012; Lenaerts et al., 2018; Datta et al., 2019) and the
505 GrIS (Lucas-Picher et al., 2012; Fettweis et al., 2017; van den Broeke et al., 2016). Further
506 statistical downscaling to 1 km resolution is required to resolve SMB over narrow GrIS outlet
507 glaciers (Noël et al., 2018a). The resulting gridded SMB products cover multiple decades
508 (1979/1958-present for AIS/GrIS, respectively) at (sub-)daily timescales, allowing synoptic
509 case studies at the SMB component level but also multidecadal trend analysis. RCM products
510 also helped to extend ice-sheet SMB time series further back in time by guiding the
511 interpolation between firn cores (Thomas et al., 2017; Box, 2013).

512 Further improvements are needed: RCMs struggle to realistically simulate (mixed-
513 phase) clouds (van Tricht et al., 2016) and (sub-) surface processes, such as drifting snow
514 (Lenaerts et al., 2017), bio-albedo (Stibal et al., 2017) and heterogeneous meltwater
515 percolation (Steger et al., 2017). A powerful emerging observational technique for dry snow
516 zones is airborne accumulation radar (Koenig et al., 2016; Lewis et al., 2017), which together
517 with improved re-analyses products such as MERRA (Cullather et al., 2016) will further
518 improve our knowledge of contemporary ice-sheet SMB.

519

520 3.4.2 Greenland

521

522 Despite considerable advances with RCMs and SMB models, there are significant remaining
523 biases in absolute values between GrIS SMB simulations for the last few decades. However,
524 these are expected to be at least partly reconciled through a new SMB Model Intercomparison
525 Project (SMB_MIP; Fettweis, 2018) which is standardising model comparisons and
526 evaluation using in-situ and satellite data (e.g. Machguth et al., 2016). The results of this
527 exercise should help to improve the models as well as inform on what are the more reliable
528 model outputs. This exercise may help to resolve significant disagreement between model
529 reconstructions of GrIS SMB, and especially accumulation, for the last 50-150 years (van den
530 Broeke et al., 2017).

531 The elevation classes downscaling method has been applied to 1850-2100 GrIS SMB
532 simulations in several studies with the Community Earth System Model (CESM): these
533 encompass regional climate and SMB projections (Vizcaino et al., 2014), a freshwater
534 forcing reconstruction and effect on ocean circulation (Lenaerts et al., 2015), the relationship
535 between SMB variability and future climate change (Fyke et al., 2014b), and the time of
536 emergence of an anthropogenic SMB signal from background SMB variability (Fyke et al.,
537 2014c). The latter study assesses the point in time when the anthropogenic trend in the SMB
538 becomes larger than the “noise”, and addresses an observational gap given the short records
539 and/or limited density of remote-sensing/in-situ observations and high GrIS SMB variability
540 (Wouters et al., 2013). Fyke et al. (2014c) identified a bimodal emergence pattern, with
541 upward emergence (positive SMB trend) in the interior due to increased accumulation,
542 downward emergence (negative SMB trend) in the margins due to increased ablation, and an
543 intermediate area of no emergence due to compensating elevated ablation and accumulation.
544 This study suggests the Greenland summit as an interesting area to monitor emergence, due
545 to its high signal-to-noise ratio and resulting early emergence. This high ratio is due to low
546 SMB variability from drier and colder conditions relative to the margins. These results should
547 be revisited with further simulations, e.g., from an ensemble and/or multiple models.
548 Additionally, they should be confronted with available observations of the recent strong SMB

549 decline to identify whether the models adequately represent the causes of this trend (e.g.,
550 Greenland Blocking, Hanna et al., 2018).

551

552 3.4.3 Antarctica

553

554 Shepherd et al. (2018) reveal that present sub-decadal to decadal precipitation and SMB
555 variations significantly dominate EAIS mass balance variability (Gardner et al., 2018)
556 justifying the need for further SMB model improvements, validations, and inter-comparisons
557 (Agosta et al., 2019; Favier et al., 2017). Thanks to observations, the inclusion of several key
558 processes have been improved in models since AR5, including the roles of the stable
559 atmospheric boundary layer (Vignon et al., 2017), drifting snow, (Amory et al., 2017; van
560 Wessem et al., 2018) and supraglacial hydrology (Kingslake et al., 2015, 2017; Hubbard et
561 al., 2016).

562 A persistent problem is that climate reanalyses used to force regional climate models
563 still present biases (Bromwich et al., 2011), most noticeably in moisture transport (Dufour et
564 al., 2019). Constraining atmospheric moisture and cloud microphysics with ground-based
565 techniques in Antarctica [ceilometer, infrared pyrometer, vertically profiling precipitation
566 radar (Gorodetskaya et al., 2015), polarimetric weather radar, micro rain radar, weighing
567 gauges, multi-angle snowflake cameras (Grazioli et al., 2017a), etc.] is necessary to
568 accurately model cloud evolution and precipitation. Ground-based estimates of cloud
569 properties and precipitation are only obtained at a few sites, which calls for the use of
570 distributed remote-sensing techniques to characterise Antarctic precipitation statistics and
571 rates [e.g., Cloudsat products (Palermé et al., 2014)]. However, processes occurring within 1
572 km above the surface remain undetected by satellite sensors. In this critical layer for SMB,
573 sublimation impacts precipitating snowflakes (Grazioli et al., 2017b) and drifting snow
574 particles (Amory et al., 2017; van Wessem et al., 2018), reducing surface accumulation and
575 leading to potential feedbacks on atmospheric moisture (Barral et al., 2014). Thus
576 continental-scale sublimation may be underestimated, suggesting mass balance and SMB
577 agreement likely relies on some degree of error compensation in models (Agosta et al., 2019).

578 Recent progress has shown that an improved description of the atmospheric structure
579 is needed during precipitation events; several studies present site-specific results on
580 precipitation origins [precipitation from synoptic scale systems, hoar frost, diamond dust
581 (Dittmann et al., 2016; Stenni et al., 2016; Schlosser et al., 2016)] and their impact on the
582 local SMB. Synoptic-scale precipitation is known to control the inter-annual variability of
583 accumulation in Dronning Maud Land (Gorodetskaya et al., 2014), Dome C, and Dome F
584 (Schlosser et al., 2016) through high-intensity precipitation events, but continental-scale
585 studies for Antarctica are still rare (Turner et al., 2019). High precipitation events are related
586 to warm and moist air mass intrusions linked to mid-tropospheric planetary waves (Turner et
587 al. 2016) that are connected with the main modes of atmospheric circulation variability at
588 southern high-latitudes (Thompson et al., 2011; Turner et al., 2016; Nicolas et al., 2017;
589 Bromwich et al., 2012). Low-elevation surface melt in West Antarctica (Nicolas et al., 2017;
590 Scott et al., 2019) and on the Larsen ice shelves (Kuipers Munneke et al., 2018; Bozkurt et
591 al., 2018) occurs during increased foehn events (Cape et al., 2015) and moisture intrusions
592 favoured by large synoptic blockings (Scott et al., 2019). These melt-related moisture
593 intrusions generally occur in the form of atmospheric rivers (Wille et al., 2019). However, the
594 synoptic causes of these events are still poorly known. Moreover, the feedbacks between
595 melting and albedo, which may be critical for processes prior to ice shelf collapse (Kingslake
596 et al., 2017; Bell et al., 2018), are poorly observed in the field. Currently, there is a major gap
597 between the large scale on which models and remote sensing typically operate (Lenaerts et
598 al., 2016; Kuipers Munneke et al., 2018) and the local scale, especially regarding snow

599 erosion and redistribution (Amory et al., 2017). These latter processes typically occur at a
600 decametre scale (Libois et al., 2014; Souverijns et al., 2018), which is not matched by space-
601 and airborne microwave radar (e.g., between 4 and 6 GHz) or ground penetrating radar
602 (GPR) (Fujita et al., 2011; Verfaillie et al., 2012; Medley et al., 2013, 2015; Frezzotti et al.,
603 2007) observations on the kilometre scale that are used to evaluate regional climate models
604 (Agosta et al., 2019; van Wessem et al., 2018).

605 Despite improvements in regional-scale models, assessing the future SMB of
606 Antarctica will rely on our capability to produce accurate future projections of the moisture
607 fluxes towards Antarctica, e.g. linked to changes in sea-ice cover (Bracegirdle et al., 2017;
608 Krinner et al., 2014; Palerme et al., 2017), and the westerly circulation and atmospheric
609 blocking patterns around Antarctica (Massom et al., 2004). These aspects are still poorly
610 represented in CMIP5 simulations (Bracegirdle et al., 2017; Favier et al., 2016). To resolve
611 this, bias corrections based on nudging approaches or data assimilation schemes have been
612 proposed, in addition to ensemble approaches (Beaumet et al., 2019; Krinner et al., 2014,
613 Krinner et al. 2019). To aid these efforts, paleo-climate information on the westerlies
614 (Saunders et al., 2018), sea ice characteristics (Campagne et al., 2015), temperature (Jones et
615 al., 2016), and SMB (Thomas et al., 2017) may be useful for constraining the models (Jones
616 et al., 2016; Abram et al., 2014) and attributing SMB changes to anthropogenic warming.
617 Emergence of this signal from the natural climate variability of Antarctica is currently
618 expected between 2020-2050 (Previdi and Polvani, 2016).

619

620 **4.0. Recent and projected mass-balance rates for glaciers and ice caps**

621

622 In this section we target valley glaciers or mountain glaciers and ice caps (<50,000 km²). We
623 here review the advances, since the IPCC AR5, in the estimate of the contribution to SLR of
624 wastage from these smaller glaciers and ice caps (henceforth, glaciers), as well as its
625 projections to the end of the 21st century. At the time of AR5, the first consensus estimate of
626 this contribution had just been published (Gardner et al., 2013), and it was estimated to be
627 $259 \pm 28 \text{ Gt yr}^{-1}$ ($0.94 \pm 0.08 \text{ mm yr}^{-1}$ SLE) for 2003–2009, including the contribution from the
628 glaciers in the periphery of Greenland and Antarctica (henceforth, peripheral glaciers). For
629 the longer period of 1993–2010, AR5 attributed 27% of the SLR to wastage from glaciers
630 (Church et al., 2013). This was above the combined contribution of the ice sheets of
631 Antarctica and Greenland (21%), despite the fact that global glacier volume is only ~0.6% of
632 the combined volume of both ice sheets (Vaughan et al., 2013). Since then, the contribution
633 to SLR from the ice sheets has accelerated, as discussed in earlier sections, which has
634 resulted in a current dominance of the ice-sheet contribution despite the contribution from
635 glaciers having also increased in absolute terms, as will be discussed in this section.

636

637 *4.1 Methods used to estimate the global glacier mass balance*

638

639 For estimating the global mass balance of glaciers, in addition to the techniques already
640 discussed for ice sheets, such as repeated altimetry (e.g. Moholdt et al., 2010), gravity
641 observations (e.g. Luthcke et al., 2008), or the mass budget method (e.g. Deschamps-Berger
642 et al., 2019), other methods are commonly used, which are sometimes variations of those
643 mentioned above. Purely observation-based techniques include the extrapolation of both in-
644 situ direct observations by the glaciological method and geodetic mass balance estimates
645 (Cogley, 2009), as well as reconstructions based on glacier length changes (Leclercq et al.,
646 2011, 2012, 2014). The glaciological method relies on point measurements of surface mass
647 balance, which are then integrated to the entire glacier surface (Cogley et al., 2011). Such
648 measurements are available for a reduced sample of <300 glaciers (Zemp et al., 2015) out of

649 more than 200,000 glaciers inventoried worldwide (Pfeffer et al., 2014), which introduces a
650 bias when extrapolating to the whole glacierized area of undersampled regions (Gardner et al,
651 2013). The geodetic mass balance, in turn, is determined using volume changes from DEM
652 differencing and then converting to mass changes using an appropriate assumption for the
653 density (Huss, 2013). The reconstructions based on observed glacier length changes convert
654 these, upon normalization and averaging to a global mean, to normalized global volume
655 change. The latter is converted into global glacier mass change using a calibration against
656 global glacier mass change over a certain period (Leclercq et al., 2011).

657 Finally, the modelling-based approaches for estimating past or current changes are
658 mostly based on the use of climatic mass balance models forced by either climate
659 observations or climate model output, calibrated and validated using surface mass-balance
660 observations. As these techniques are based on a statistical scaling relationship, they are
661 commonly referred to as statistical modelling, to distinguish them from the use of an RCM to
662 estimate, directly, the surface mass balance of an ice mass. The latter works well for ice caps,
663 but not for glaciers, due to their complex topography and corresponding micro-climatological
664 effects (Bamber et al., 2018). Based on statistical modelling, an analysis of the processes and
665 feedbacks affecting the global sensitivity of glaciers to climate change can be found in
666 Marzeion et al. (2014a), while the attribution of the observed mass changes to anthropogenic
667 and natural causes has been addressed by Marzeion et al. (2014b).

668

669 *4.2 20th century and current estimates*

670

671 Much of the work done since AR5 has focused on improving the estimates for the reference
672 period 2003-2009 (or some earlier periods), and on producing new estimates for more recent
673 (or extended) periods. Both the reanalyses and the new estimates have been based on
674 improvements in the number of mass balance or glacier length changes observations, and on
675 the use of an increased set of gridded climate observations, and of more complete and
676 accurate global glacier inventories and global DEMs. These improvements allowed Marzeion
677 et al. (2015) to achieve the agreement, within error bounds, of the global reconstructions of
678 the mass losses from glacier wastage for the periods 1961-2005, 1902-2005 and 2003-2009
679 produced using the various methods available. In spite of the agreement at the global level,
680 strong disagreements persisted for particular regions such as Svalbard and the Canadian
681 Arctic, likely because of the omission of calving in the statistical models. Marzeion et al.
682 (2017), using a yet more extended set of glaciological and geodetic measurements (Zemp et
683 al., 2015), gave a global glacier mass-change rate estimate of -0.61 ± 0.07 mm SLE yr^{-1} for
684 2003-2009 (including Greenland peripheral glaciers, but not those of the Antarctic
685 periphery), obtained by averaging various recent GRACE-based studies (Jacob et al., 2012;
686 Chen et al., 2013; Yi et al., 2015; Schrama et al., 2014) and several studies combining
687 GRACE with other datasets (Gardner et al., 2013, and an update of it; Dieng et al., 2015;
688 Reager et al., 2016; Rietbroek et al., 2016). The studies based on GRACE data consistently
689 give less negative glacier mass balances than those obtained using other methods.
690 Uncertainties in the GRACE-derived estimates remain important especially due to the small
691 size of glaciers compared with the GRACE footprint of ~ 300 km. Associated problems
692 include the leakage of the gravity signal into the oceans, or the difficulty of distinguishing
693 between mass changes due to glacier mass changes or to land water storage changes. In
694 regional and global studies, however, the problem of the footprint and related leakage is not
695 relevant, as individual glaciers need not to be resolved and GRACE has been shown to be
696 effective in providing measurements of mass changes for clusters of glaciers (Luthcke et al.,
697 2008). Uncertainties in the GIA correction also remain, and the effects of rebound from the
698 Little Ice Age (LIA) deglaciation have to be accounted for.

699 Parkes and Marzeion (2018) have analysed the contribution to SLR from uncharted
700 glaciers (glaciers melted away and small glaciers not inventoried) during the 21st century.
701 Although they will play a minimal role in SLR in the future, the important finding is that their
702 contribution is sufficient to close the historical sea-level budget, for which undiscovered
703 physical processes are then no longer required.

704 Bamber et al. (2018) have updated the glacier mass-change rates presented in
705 Marzeion et al. (2017) by adding new estimates of mass trends for the Arctic glaciers and ice
706 caps and the glaciers of High-Mountain Asia and Patagonia, which together contribute to
707 84% of the SLR from glacier wastage. They combine the most recent observations (including
708 CryoSat2 radar altimetry) and the latest results from statistical modelling, as well as regional
709 climate modelling for the Arctic ice caps (Noël et al., 2018b) and stereo photogrammetry for
710 High-Mountain Asia (Brun et al., 2017). They find poor agreement between the estimates
711 based on statistical modelling and all other methods (altimetry/gravimetry/RCM) for Arctic
712 Canada, Svalbard, peripheral Greenland, the Russian Arctic and the Andes, which are all
713 regions with significant marine- or lake-terminating glaciers, where statistical modelling,
714 which does not account for frontal ablation, is expected to perform worse than the
715 observational-based approaches. Bamber et al. (2018) also present pentadal mass balance
716 rates for the period 1992-2016, which are shown in **Table 2** and clearly illustrate the increase
717 in global glacier mass losses. If we add to the mass budget for the last pentad (2012-2016) in
718 **Table 2** the mass budget of -33 Gt yr^{-1} for the Greenland peripheral glaciers estimated by
719 averaging the CryoSat and RCM values for 2010-2014 given in Table 1 of Bamber et al.
720 (2018), and the mass budget of -6 Gt yr^{-1} for the Antarctic peripheral glaciers over 2003-
721 2009 estimated by Gardner et al. (2013), we get an estimate of the current global glacier
722 mass budget of $-266 \pm 33 \text{ Gt yr}^{-1}$ ($0.73 \pm 0.09 \text{ mm SLE yr}^{-1}$).

723 The most recent studies to highlight are those of Zemp et al. (2019) and Wouters et al.
724 (2019). The former is based on glaciological and geodetic measurements but uses a much-
725 extended dataset (especially for the geodetic measurements), the most updated glacier
726 inventory (RGI 6.0) and a novel approach. The latter combines, for each glacier region, the
727 temporal variability from the glaciological sample with the glacier-specific values of the
728 geodetic sample. The calibrated annual time series is then extrapolated to the whole set of
729 regional glaciers to assess regional mass changes, considering the rates of area change in the
730 region. The authors claim that this procedure has overcome the earlier reported negative bias
731 in the glaciological sample (Gardner et al., 2013). Nevertheless, for large glacierised regions
732 (e.g. RGI regions), large differences remain between different mass-loss estimates, for
733 example in the Southern Andes where two recent studies have found reduced mass loss
734 compared to Zemp et al. (2019) and Wouters et al. (2019) using differencing of digital
735 elevation models (Braun et al., 2019; Dussaillant et al., 2019). However, the global glacier
736 mass loss estimate by Zemp et al. (2019), of $0.74 \pm 0.05 \text{ mm SLE yr}^{-1}$ during 2006-2016,
737 excluding the peripheral glaciers ($0.92 \pm 0.39 \text{ mm SLE yr}^{-1}$ if included), is still large compared
738 to that by Bamber et al. (2018), of $0.59 \pm 0.11 \text{ mm SLE yr}^{-1}$ for the same period, which is very
739 similar to the most recent gravimetry-based estimate by Wouters et al. (2019), of 0.55 ± 0.10
740 mm SLE yr^{-1} , again for the same period (from their Table S1). This estimate is an
741 improvement over earlier ones, by using longer time series, an updated glacier inventory
742 (RGI 6.0), the latest GRACE releases (RL06), which are combined in an ensemble to further
743 reduce the noise, a new GIA model (Caron et al., 2018) and new hydrology models (GLDAS
744 V2.1 (Rodell et al., 2004; Beaudoin and Rodell, 2016), and PCR-GLOBW 2 (Sutanudjaja et
745 al., 2018)) to remove the signal from continental hydrology.

746
747
748

749 4.3 Projected estimates to the end of the 21st century

750

751 Among the post-AR5 studies on projected global estimates of mass losses by glaciers to the
752 end of the 21st century, we highlight those of Radić et al. (2014), Huss and Hock (2015) and
753 Marzeion et al. (2018), together with the main results from the recent model intercomparison
754 by Hock et al. (2019). An account of other pre- and post-AR5 (up to 2016) projections can be
755 found in the review by Slangen et al. (2017). While the first two mentioned projections share
756 many common features (glacier inventory, global climate models and emission scenarios, a
757 temperature-index mass balance model, similar climate forcing for the calibration period and
758 similar global DEMs), they have two remarkable differences. First, Radić et al. (2014) rely on
759 volume-area scaling for the initial volume estimate and to account for the dynamic response
760 to modelled mass change, while Huss and Hock (2015) derive the initial ice-thickness
761 distribution using the inverse method by Huss and Farinotti (2012), and the modelled glacier
762 dynamic response to mass changes is based on an empirical relation between thickness
763 change and normalized elevation range (Huss et al., 2010). Second, the Huss and Hock
764 (2015) model accounts for frontal ablation of marine-terminating glaciers, dominated by
765 calving losses and submarine melt. The results by Radić et al. (2014) suggest SLR
766 contributions of 155 ± 41 (RCP4.5) and 216 ± 44 (RCP8.5) mm, similar to the projections of
767 Marzeion et al. (2012), and to the projections of Slangen and van de Wal (2011) updated in
768 Slangen et al. (2017). However, the more updated and complete model by Huss and Hock
769 (2015) predicts lower contributions, of 79 ± 24 (RCP2.6), 108 ± 28 (RCP4.5), and 157 ± 31
770 (RCP8.5) mm. Of these glacier mass losses, ~10% correspond to frontal ablation globally,
771 and up to ~30% regionally. In both models, the most important contributors to SLR are the
772 Canadian Arctic, Alaska, the Russian Arctic, Svalbard, and the periphery of Greenland and
773 Antarctica. Both models are highly sensitive to the initial ice volume. Regarding Marzeion et
774 al. (2018), while they use basically the same statistical model as in Marzeion et al. (2012,
775 2014a,b, 2015, 2017), the use of a newer version (5.0) of the RGI, as well as updated DEMs
776 and SMB calibration datasets, led to lower SLR contributions from glacier wastage to the end
777 of the 21st century, similar to those by Huss and Hock (2015): 84 [54–116] (RCP2.6), 104
778 [58–136] (RCP4.5) and 142 [83–165] (RCP8.5) mm (the numbers in brackets indicate the
779 fifth and ninety-fifth percentiles of the glacier model ensemble distribution).

780 A recent intercomparison of six global-scale glacier mass-balance models,
781 GlacierMIP (Hock et al., 2019), has provided a total of 214 projections of annual glacier mass
782 and area, to the end of the 21st century, forced by 25 GCMs and four RCPs. Global glacier
783 mass loss (including Greenland and Antarctic peripheries) by 2100 relative to 2015, averaged
784 over all model runs, varies between 94 ± 25 (RCP2.6) and 200 ± 44 (RCP8.5) mm SLE. Large
785 differences are found between the results from the various models even for identical RCPs,
786 particularly for some glacier regions. These discrepancies are attributed to differences in
787 model physics, calibration and downscaling procedures, input data and initial glacier volume,
788 and the number and ensembles of GCMs used.

789 Although only a regional study, the modelling by Zekollari et al. (2019) is a good
790 example of one of the lines of improvements expected for the future generation of models for
791 projecting the future evolution of glaciers. Zekollari et al. (2019) have added ice dynamics to
792 the model by Huss and Hock (2015), in which glacier changes are imposed based on a
793 parameterization of the changes in surface elevation at a regional scale. The inclusion of ice
794 dynamics results in a reduction of the projected mass loss, especially for the low-emission
795 scenarios such as RCP2.6, and this effect increases with the glacier elevation range, which is
796 typically broader for the largest glaciers.

797 The contribution from glaciers to SLR is expected to continue to increase during most
798 of the 21st century. Note e.g. that the projections by Huss and Hock (2015) give average rates,

799 over their 90-yr modelled period, between 0.88 ± 0.27 and 1.74 ± 0.34 mm SLE yr^{-1} , depending
800 on the emission scenario, which are larger than the current rates. However, this contribution
801 is expected to decay as the total ice volume stored in glaciers becomes smaller as the low-
802 latitude and low-altitude glaciers disappear and those remaining become confined to the
803 higher latitudes and altitudes. The projections by Huss and Hock (2015) yield a global glacier
804 volume loss of 25–48% between 2010 and 2100, depending on the scenario. In parallel, the
805 contribution from the ice sheets is increasing (e.g. Shepherd et al., 2013, 2018; this paper),
806 and thus the sea-level rise caused by mass losses from land ice masses will more and more be
807 dominated by losses from the ice sheets (**Table 3**).

808

809 **5.0 Summary and outlook**

810

811 Never before have there been so much new observational, especially satellite, data for
812 assessing the state of mass balance of ice sheets and glaciers and their sensitivity to ongoing
813 climate change. However, the usable satellite record is still relatively short in climate terms.
814 One of the main remaining challenges is that satellite observations date back only 2-3
815 decades, which is a very short period for the reference and evaluation of century-scale
816 projections. Therefore, further extension of the ice-sheet satellite record into the past, for
817 example through revised processing of earlier albeit lower quality observations following the
818 method of Trusel et al. (2018), would greatly inform modellers. Also in the same line, and for
819 the sake of ice-sheet mass and regional climate change detection and attribution, model
820 evaluation and improved projections, the maintenance and extension of current automatic
821 weather stations (e.g. Hermann et al., 2018; Smeets et al. 2018) across the ice sheets is of key
822 interest, with particular emphasis on energy balance stations able to quantify melt energy.

823 Our review highlights that, despite recent efforts, significant discrepancies remain
824 with respect to absolute mass balance values for the EAIS, and so further studies are
825 recommended to resolve this matter. Compared to the AIS, for the GrIS, there is a higher
826 level of agreement, but absolute values vary by $\sim 100\text{--}300$ Gt yr^{-1} between recent years. These
827 significant fluctuations are mainly due to SMB variability (precipitation and runoff) that are
828 in turn linked to fluctuations in atmospheric circulation. Ice dynamics may also have an
829 important role to play in future changes of the GrIS, especially in regions away from the
830 southwest, and the relative contributions of SMB and dynamics to future mass change remain
831 unclear.

832 Continued monitoring is vital to resolve these open questions. Apart from ensuring
833 the continuity of key satellite data provided by missions including GRACE Follow On
834 (gravimetry) and ICESat2 (altimetry), and carrying out more frequent (annual)
835 comprehensive inter-comparison assessments of ice-sheet mass balance, the cryospheric and
836 climate science communities need to enhance existing collaborations on improving regional
837 climate model and SMB simulations of Antarctica and Greenland (SMB_MIP being a key
838 example), and also make further significant improvements to GIA models, as these are some
839 of the key sources of residual uncertainty underlying current ice-sheet mass balance
840 estimates.

841 Recent advances in ice-sheet models show major improvements in terms of
842 understanding of physics and rheology and model initialization, especially thanks to the
843 wealth of satellite data that has recently become available. However, recent model
844 intercomparisons (Goelzer et al., 2018a; Seroussi et al., 2019) still point to large process and
845 parameter uncertainties. Nevertheless, new techniques need to be further explored to improve
846 initialization methods using both surface elevation and ice velocity changes, allowing for
847 improved understanding of underlying friction laws and rheological conditions of marine-
848 terminating glaciers (e.g. Gillet-Chaulet et al., 2016; Gillet-Chaulet, 2019). Given that marine

849 outlet glaciers are especially sensitive to small-change topographic variations, multi-
850 parameter ensemble modelling and the use of novel emulation methods to evaluate
851 uncertainty will become an essential tool in ice-sheet modelling. There is a corresponding
852 need to acquire additional high resolution subglacial topography data to help with
853 predictions. Several paleo-studies have also emphasized the importance of subglacial
854 topography in controlling grounding zone location. Jamieson et al. (2012), Batchelor and
855 Dowdeswell (2015), and Danielson and Bart (2019) all demonstrate that the post-LGM
856 Antarctic grounding line preferentially stabilized in regions where there are vertical or lateral
857 topographic restrictions. Meanwhile, in recognition of the remaining limitations of ice-sheet
858 models, despite significant recent progress, alternative novel approaches including structured
859 expert judgment are useful to assess the likely impact of ongoing ice-sheet melt on SLR. For
860 example, Bamber et al. (2019) indicate that a high-emissions greenhouse warming scenario
861 gives a not insignificant chance of a total >2 m SLR by 2100.

862 Regarding glaciers other than the ice sheets, in spite of recent improvements the
863 observational database needs to be further extended in space and time. As suggested by Zemp
864 et al. (2019), emphasis should be on closing data gaps in: 1) regions where glaciers dominate
865 runoff during warm/dry seasons (tropical Andes and Central Asia), and 2) regions expected to
866 dominate the future glacier contribution to SLR (Alaska, Arctic Canada, the Russian Arctic
867 and Greenland and Antarctica peripheries). ICESat-2 and GRACE follow-on missions are
868 likely to have revolutionary impacts on our knowledge of the mass changes of glaciers and
869 ice caps, though GIA corrections and LIA deglaciation effects still have room for
870 improvement. ICESat-2 especially, with its multiple laser beams and precise repeat-track
871 pointing capability, has the potential to revolutionise our knowledge of mass changes on
872 small glaciers worldwide. However, there is an unfortunate conflict that is seriously limiting
873 ICESat-2 collection of precise repeat-track data globally. The current mission operation for
874 ICESat-2 has systematic off-nadir pointing outside of polar regions to provide denser
875 mapping of vegetation biomass for a vegetation inventory, despite the fact that such data is
876 also being collected by the GEDI laser altimeter on the International Space Station. After one
877 year of ICESat-2 vegetation-inventory mapping, it would be advisable that the mission
878 operation plan be changed to precise-repeat track pointing to reference tracks globally for
879 studies of mass changes of glaciers and ice caps, which will also provide improved vegetation
880 measurements for studies of seasonal and interannual vegetation changes. DEM differencing
881 from sub-metre resolution optical satellites such as Quickbird, WorldView and Pléiades will
882 play a key role in geodetic mass-balance estimates (Kronenberg et al. 2016; Melkonian et al.,
883 2016; Berthier et al., 2014). The discrepancy between the GlacierMIP mass-change
884 projections from the various models, even under identical emission scenarios, calls for further
885 standardized intercomparison experiments, where common glacier inventory version, initial
886 glacier volume, ensemble of GCMs and RCP emission scenarios are prescribed for all models
887 (Hock et al., 2019). Finally, projections of future contributions to SLR will benefit from
888 inclusion in the models of ice dynamics, as done by Zekollari et al. (2019).

889

890 **Acknowledgements**

891

892 The authors are grateful to WCRP CliC, SCAR and IASC for sponsoring the ISMASS
893 workshop in Davos, Switzerland, on 15 June 2018 that led to this paper. FN received funding
894 from grant CTM2017-84441-R of the Spanish State Plan for R&D. KB acknowledges
895 support from the Fonds de la Recherche Scientifique de Belgique (F.R.S.-FNRS). HG
896 received funding from the programme of the Netherlands Earth System Science Centre
897 (NESSC), financially supported by the Dutch Ministry of Education, Culture and Science
898 (OCW) under grant no. 024.002.001. MV acknowledges support from the European Research

899 Council ERC-StG-678145-CoupledIceClim. EH thanks Jay Zwally for permission to
900 reproduce Figure 1, and Holly Garner for help with final checking.

901
902
903
904
905
906
907
908
909
910
911
912
913
914
915
916
917
918
919
920
921
922
923
924
925
926
927
928
929
930
931
932
933
934
935
936
937
938
939
940
941
942
943
944
945
946
947
948

949 **References**

950

951 Abram, N.J., Mulvaney, R., Vimeux, F., Phipps, S.J., Turner, J., England, M.H., 2014.
952 Evolution of the Southern Annular Mode during the past millennium. *Nat. Clim. Change* 4,
953 564–569, doi:10.1038/nclimate2235.

954

955 Adhikari, S., Ivins, E.R., Larour, E., Seroussi, H., Morlighem, M., Nowicki, S., 2014. Future
956 Antarctic bed topography and its implications for ice sheet dynamics. *Solid Earth* 5, 569-584.

957

958 Agosta, C., Amory, C., Kittel, C., Orsi, A., Favier, V., Gallée, H., van den Broeke, M.R.,
959 Lenaerts, J.T.M., van Wessem, J.M., Fettweis, X., 2019. Estimation of the Antarctic surface
960 mass balance using the regional climate model MAR (1979–2015) and identification of
961 dominant processes, *The Cryosphere* 13, 281-296.

962

963 Alexander, P. M., LeGrande, A. N., Fischer, E., Tedesco, M., Fettweis, X., Kelley, M.,
964 Nowicki, S. M. J., Schmidt, G. A., 2019. Simulated Greenland surface mass balance in the
965 GISS ModelE2 GCM: Role of the ice sheet surface. *Journal of Geophysical Research: Earth*
966 *Surface* 124, 750–765.

967

968 Amory, C., Gallée, H., Naaim-Bouvet, F., Favier, V., Vignot, E., Picard, G., Trouvillez, A.,
969 Picard, L., Genthon, C., Bellot, H., 2017. Seasonal Variations in Drag Coefficient over a
970 Sastrugi-Covered Snowfield in Coastal East Antarctica. *Bound.-Layer Meteorol.* 164, 107-
971 133.

972

973 Andersen, M.L., Stenseng, L., Skourup, H., Colgan, W., Khan, S.A., Kristensen, S.S.,
974 Andersen, S.B., Box, J.E., Ahlstrøm, A.P., Fettweis, X., Forsberg, R., 2015. Basin-scale
975 partitioning of Greenland ice sheet mass balance components (2007-2011). *Earth Planet. Sci.*
976 *Lett.* 409, 89-95.

977

978 Argus, D.F., Peltier, W.R., Drummond, R., Moore, A.W., 2014. The Antarctica component of
979 postglacial rebound model ICE-6G_C (VM5a) based on GPS positioning, exposure age
980 dating of ice thicknesses, and relative sea level histories. *Geophysical Journal International*
981 198(1), 537-563.

982

983 Arthern, R.J., Gudmundsson G.H., 2010. Initialization of ice-sheet forecasts viewed as an
984 inverse Robin problem. *J. Glaciol.* 56 (197), 527–33, doi:10.3189/002214310792447699.

985

986 Arthern, R.J., Hindmarsh, R.C.A., 2006. Determining the contribution of Antarctica to sea-
987 level rise using data assimilation methods. *Philos. Transact. A Math. Phys. Eng. Sci.*
988 364(1844):1841–65, doi:10.1098/rsta.2006.1801.

989

990 Arthern, R.J., Winebrenner, D.P., Vaughan, D.G., 2006. Antarctic snow accumulation
991 mapped using polarization of 4.3-cm wavelength microwave emission. *J. Geophys. Res.*
992 *Atmos.* 111(6):1-10. doi:10.1029/2004JD005667.

993

994 Asay-Davis, X. S., Jourdain, N.C., and Nakayama, Y., 2017. Developments in Simulating
995 and Parameterizing Interactions Between the Southern Ocean and the Antarctic Ice Sheet.
996 *Curr. Clim. Change Rep.* 3, 316–329, doi:10.1007/s40641-017-0071-0.

997

998 Bales, R.C., Guo, Q., Shen, D., McConnell, J.R., Du., G., Burkhart, J.F., Spikes, V.B.,

999 Hanna, E., Cappelen, J., 2009. Annual accumulation for Greenland updated using ice core
1000 data developed during 2000-2006 and analysis of daily coastal meteorological data. *J.*
1001 *Geophys. Res. Atmos.* 114(6), D06116, doi:10.1029/2008JD011208.
1002

1003 Bamber, J.L., Westaway, R.M., Marzeion, B., Wouters, B., 2018. The land ice contribution to
1004 sea level during the satellite era. *Environmental Research Letters* 13, 063008.
1005 doi:10.1088/1748-9326/aac2f0.
1006

1007 Bamber, J.L., Oppenheimer, M., Kopp, R.E., Aspinall, W.P., Cooke, R.M., 2019. Ice sheet
1008 contributions to future sea-level rise from structured expert judgment. *PNAS* 116 (23),
1009 11195-11200, <https://doi.org/10.1073/pnas.1817205116>.
1010

1011 Barletta, V.R., Bevis, M., Smith, B.E., Wilson, T., Brown, A., Bordoni, A., Willis, M., Khan,
1012 S.A., Rovira-Navarro, M., Dalziel, I., Smalley, R., Kendrick, E., Konfal, S., Caccamise, D.J.,
1013 Aster, R.C., Nyblade, A., Wiens, D.A., 2018. Observed rapid bedrock uplift in Amundsen
1014 Sea Embayment promotes ice-sheet stability. *Science*, 360(6395): 1335-1339.
1015

1016 Barral, H., Genthon, C., Trouvilliez, A., Brun, C., Amory, C., 2014. Blowing snow in coastal
1017 Adélie Land, Antarctica: three atmospheric-moisture issues. *The Cryosphere* 8, 1905–1919,
1018 doi:10.5194/tc-8-1905-2014.
1019

1020 Bart, P.J., DeCesare, M., Rosenheim, B.E., Majewski, W., McGlannan, A., 2018. A
1021 centuries-long delay between a paleo-ice-shelf collapse and grounding-line retreat in the
1022 Whales Deep Basin, eastern Ross Sea, Antarctica. *Scientific Reports* 8, 12392.
1023

1024 Bassis, J.N., Walker, C.C., 2012. Upper and lower limits on the stability of calving glaciers
1025 from the yield strength envelope of ice. *Proc. R. Soc. Lond. A Math. Phys. Sci.*
1026 468(2140):913–31. doi:10.1098/rspa.2011.0422
1027

1028 Batchelor, C.L., Dowdeswell, J.A., 2015. Ice-sheet grounding-zone wedges (GZWs) on high-
1029 latitude continental margins. *Marine Geology* 363, 65-92.
1030

1031 Baur, O., Kuhn, M., Featherstone, W.E., 2013. Continental mass change from GRACE over
1032 2002-2011 and its impact on sea level. *Journal of Geodesy*, 87(2): 117-125.
1033

1034 Beaudoin, H., Rodell, M., 2016. GLDAS Noah Land Surface Model L4 monthly 0.25 x 392
1035 0.25 degree V2.1, doi:10.5067/SXAVCZFAQLNO.
1036

1037 Beaumet, J., Krinner, G., Déqué, M., Haarsma, R., Li, L., 2019. Assessing bias-corrections of
1038 oceanic surface conditions for atmospheric models. *Geosci. Model Dev.* 12, 321-342.
1039 doi:<https://doi.org/10.5194/gmd-2017-247>.
1040

1041 Bell, R.E., Banwell, A.F., Trusel, L.D., Kingslake, J., 2018. Antarctic surface hydrology and
1042 impacts on ice-sheet mass balance. *Nature Climate Change* 8, 1044–1052.
1043

1044 Berthier, E., Vincent, C., Magnússon, E., Gunnlaugsson, Á.P., Pitte, P., Le Meur, E.,
1045 Masiokas, M., Ruiz, L., Pálsson, F., Belart, J.M.C., Wagnon, P., 2014. Glacier topography
1046 and elevation changes derived from Pléiades submeter stereo images. *The Cryosphere* 8,
1047 2275–2291. doi:10.5194/tc-8-2275-2014.
1048

1049 Bevis, M., Harig, C., Khan, S.A., Brown, A., Simons, F.J., Willis, M., Fettweis, X., van den
1050 Broeke, M.R., Madsen, F.B., Kendrick, E., Caccamise II, D.J., Van Dam, T., Knudsen, P.,
1051 Nylen, T., 2019. Accelerating changes in ice mass within Greenland, and the ice sheet's
1052 sensitivity to atmospheric forcing. *PNAS* 116, 1934-1939.
1053
1054 Bigg, G.R., Wei, H.L., Wilton, D.J., Zhao, Y., Billings S.A., Hanna, E., Kadiramanathan V.,
1055 2014. A century of variation in the dependence of Greenland iceberg calving on ice sheet
1056 surface mass balance and regional climate change. *Proceedings of the Royal Society A:
1057 Mathematical, Physical and Engineering Sciences* 470, 20130662.
1058
1059 Box J.E., 2013. Greenland ice sheet mass balance reconstruction. Part II: Surface mass
1060 balance: 1840-2010. *J. Clim.* 26(18), 6974-6989, doi:10.1175/JCLI-D-12-00518.1.
1061
1062 Box, J.E., Colgan, W.T., Wouters, B., Burgess, D.O., O'Neel, S., Thomson, L.I., Mernild,
1063 S.H., 2018. Global sea-level contribution from Arctic land ice: 1971-2017. *Environ. Res.
1064 Lett.* 13, 125012.
1065
1066 Bozkurt, D., Rondanelli, R., Marín, J.C., Garreaud, R., 2018. Foehn Event Triggered by an
1067 Atmospheric River Underlies Record-Setting Temperature Along Continental Antarctica. *J.
1068 Geophys. Res. Atmos.* 123, 3871–3892, doi:10.1002/2017JD027796.
1069
1070 Bracegirdle, T.J., Hyder, P., Holmes, C.R., 2017. CMIP5 Diversity in Southern Westerly Jet
1071 Projections Related to Historical Sea Ice Area: Strong Link to Strengthening and Weak Link
1072 to Shift. *J. Clim.* 31, 195–211, doi:10.1175/JCLI-D-17-0320.1.
1073
1074 Braun, M. H., Malz, P., Sommer, C., Farías-Barahona, D., Sauter, T., Casassa, G., Soruco,
1075 A., Skvarca, P., and Seehaus, T. C., 2019. Constraining glacier elevation and mass changes in
1076 South America. *Nature Climate Change* 9, 130.

1077 Bromwich, D.H., Nicolas, J.P., Monaghan, A.J., 2011. An Assessment of Precipitation
1078 Changes over Antarctica and the Southern Ocean since 1989 in Contemporary Global
1079 Reanalyses. *J. Clim.* 24, 4189–4209, doi:10.1175/2011JCLI4074.1.
1080
1081 Bromwich, D.H., Nicolas, J.P., Monaghan, A.J., Lazzara, M.A., Keller, L.M., Weidner, G.A.,
1082 Wilson, A.B., 2012. Central West Antarctica among the most rapidly warming regions on
1083 Earth. *Nat. Geosci.* 6, 139–145, doi:10.1038/ngeo1671.
1084
1085 Brun, F., Berthier, E., Wagnon, P., Käab, A., Treichler D., 2017. A spatially resolved
1086 estimate of High Mountain Asia glacier mass balances from 2000–2016. *Nature Geoscience*
1087 10(9), 668–673, doi:10.1038/NGEO2999.
1088
1089 Bulthuis, K., Arnst, M., Sun, S., Pattyn, F. 2019. Uncertainty quantification of the multi-
1090 centennial response of the Antarctic ice sheet to climate change. *The Cryosphere* 13, 1349-
1091 1380, <https://doi.org/10.5194/tc-13-1349-2019>.
1092
1093 Campagne, P., Crosta, X., Houssais, M.N., Swingedouw, D., Schmidt, S., Martin, A.,
1094 Devred, E., Capo, S., Marieu, V., Closset, I., Massé, G., 2015. Glacial ice and atmospheric
1095 forcing on the Mertz Glacier Polynya over the past 250 years. *Nat. Commun.* 6, 6642,
1096 doi:10.1038/ncomms7642.
1097

1098 Cape, M.R., Vernet, M., Skvarca, P., Marinsek, S., Scambos, T. Domack, E., 2015. Foehn
1099 winds link climate-driven warming to ice shelf evolution in Antarctica. *J. Geophys. Res.*
1100 *Atmospheres* 120, 11037-11057.
1101

1102 Caron, L., Ivins, E., Larour, E., Adhikari, S., Nilsson, J., Blewitt, G., 2018. GIA Model
1103 Statistics for Cape, GRACE Hydrology, Cryosphere, and Ocean Science. *Geophysical*
1104 *Research Letters* 45, 2203–2212, doi:10.1002/2017GL076644.
1105

1106 Chen, J.L., Wilson, C.R., Tapley, B.D., 2013. Contribution of ice sheet and mountain glacier
1107 melt to sea level rise. *Nature Geoscience* 6, 549–552, doi:10.1038/NGEO1829.
1108

1109 Christianson, K., Bushuk, M., Dutrieux, P., Parizek, B.R., Joughin, I.R., Alley, R.B., Shean,
1110 D.E., Abrahamsen, E.P., Anandakrishnan, S., Heywood, K.J., Kim, T.-W., Lee, S.-H.,
1111 Nicholls, K., Stanton, T., Truffer, M., Webber, B.G.M., Jenkins, A., Jacobs, S., Bindschadler,
1112 R., Holland, D.M., 2016. Sensitivity of Pine Island Glacier to observed ocean forcing,
1113 *Geophys. Res. Lett.*, 43, 10,817–10,825, doi:10.1002/2016GL070500.
1114

1115 Church, J.A., Clark, P.U., Cazenave, A., Gregory, J.M., Jevrejeva, S., Levermann, A.,
1116 Merrifield, M.A., Milne, G.A., Nerem, R.S., Nunn, P.D., Payne, A.J., Pfeffer, W.T.,
1117 Stammer, D., and Unnikrishnan, A.S., 2013: Sea Level Change, in: Stocker, T.F., Qin, D.,
1118 Plattner, G.-K., Tignor, M., Allen, S.K., Boschung, J., Nauels, A., Xia, Y., Bex, V., Midgley,
1119 P.M. (Eds.), *Climate Change 2013: The Physical Science Basis. Contribution of Working*
1120 *Group I to the Fifth Assessment Report of the Intergovernmental Panel on Climate Change.*
1121 Cambridge University Press, Cambridge, United Kingdom and New York, NY, USA, pp.
1122 1137–1216.
1123

1124 Citterio, M., van As, D., Ahlstrøm A.P., Andersen, M.L., Andersen, S.B., Box, J.E.,
1125 Charalampidis, C., Colgan, W.T., Fausto, R.S., Nielsen, S., Veicherts, M., 2015. Automatic
1126 weather stations for basic and applied glaciological research. *Geol. Surv. Denmark Greenl.*
1127 *Bull.* 33, 69-72. http://www.geus.dk/media/10888/nr33_p69-72.pdf.
1128

1129 Cogley, J.G., 2009. Geodetic and direct mass-balance measurements: comparison and joint
1130 analysis. *Annals of Glaciology* 50, 96–100. doi:10.3189/172756409787769744.
1131

1132 Cogley, J.G., Hock, R., Rasmussen, L.A., Arendt, A.A., Bauder, A., Braithwaite, R.J.,
1133 Jansson, P., Kaser, G., Möller, M., Nicholson, L., and Zemp, M., 2011. Glossary of Glacier
1134 Mass Balance and Related Terms. IHP-VII Technical Documents in Hydrology No. 86, IACS
1135 Contribution No. 2, UNESCO-IHP, Paris, 114 pp.
1136

1137 Cornford, S.L., Martin, D.F., Graves, D.T., Ranken, D.F., Le Brocq, A.M., Gladstone, R.M.,
1138 Payne, A.J., Ng, E.G., Lipscomb, W.H., 2013. Adaptive mesh, finite volume modeling of
1139 marine ice sheets. *J. Comput. Phys.* 232, 529–549, doi:10.1016/j.jcp.2012.08.037
1140

1141 Cornford, S.L., Martin, D.F., Payne, A.J., Ng, E.G., Le Brocq, A.M., Gladstone, R.M.,
1142 Edwards, T.L., Shannon, S.R., Agosta, C., Van Den Broeke, M.R., Hellmer, H.H., Krinner,
1143 G., Ligtenberg, S.R.M., Timmermann, R., Vaughan, D.G., 2015. Century-scale simulations
1144 of the response of the West Antarctic Ice Sheet to a warming climate. *Cryosphere* 9(4), 1579–
1145 600, doi:10.5194/tc-9-1579-2015.
1146

1147 Cornford, S.L., Martin, D.F., Lee, V., Payne, A.J., Ng, E.G., 2016. Adaptive mesh refinement
1148 versus subgrid friction interpolation in simulations of Antarctic ice dynamics. *Ann. Glaciol.*
1149 57(73), 1–9, doi:10.1017/aog.2016.13.
1150

1151 Csatho, B.M., Schenk, A.F., Van der Veen, C.J., Babonis, G., Duncan, K., Rezvanbehbahani,
1152 S., Van den Broeke, M.R., Simonsen, S.B., Nagarajan, S., Van Angelen, J.H., 2014. Laser
1153 altimetry reveals complex pattern of Greenland Ice Sheet dynamics. *Proceedings of the*
1154 *National Academy of Sciences of the United States of America*, 111(52): 18478-18483.
1155

1156 Cullather, R.I., Nowicki, S.M.J., Zhao, B., Suarez, M.J., 2014. Evaluation of the Surface
1157 Representation of the Greenland Ice Sheet in a General Circulation Model. *J. Clim.* 27(13),
1158 4835-4856.
1159

1160 Cullather, R.I., Nowicki, S.M.J., Zhao, B., Koenig, L.S., 2016. A Characterization of
1161 Greenland Ice Sheet Surface Melt and Runoff in Contemporary Reanalyses and a Regional
1162 Climate Model. *Front Earth Sci.* 4: 10, doi:10.3389/feart.2016.00010.
1163

1164 Danielson, M., Bart, P.J., 2019. Topographic control on the post-LGM grounding zone
1165 locations of the West Antarctic Ice Sheet in the Whales Deep Basin, eastern Ross Sea.
1166 *Marine Geology* 407, 248-260.
1167

1168 Datta, R. T., Tedesco, M., Fettweis, X., Agosta, C., Lhermitte, S., Lenaerts, J. T.M., &
1169 Wever, N. (2019) The effect of Foehn-induced surface melt on firn evolution over the
1170 northeast Antarctic peninsula. *Geophysical Research Letters* 46, 3822–3831.
1171

1172 Davis, C. H., Ferguson, A.C., 2004. Elevation Change of the Antarctic Ice Sheet, 1995–2000,
1173 From ERS-2 Satellite Radar Altimetry. *IEEE Transactions on Geoscience and Remote*
1174 *Sensing.* 42: 2437 - 2445.
1175

1176 DeConto, R.M., Pollard, D., 2016. Contribution of Antarctica to past and future sea-level rise.
1177 *Nature* 531(7596), 591–597, doi:10.1038/nature17145.
1178

1179 Deschamps-Berger, C., Nuth, C., van Pelt, W., Berthier, E., Kohler, J., Altena, B., 2019.
1180 Closing the mass budget of a tidewater glacier: the example of Kronebreen, Svalbard. *J.*
1181 *Glaciol.*, 65(249), 136-148, doi:10.1017/jog.2018.98.
1182

1183 Dieng, H.N., Champollion, N., Cazenave, A., Wada, Y., Schrama, E., Meyssignac, B., 2015.
1184 Total land water storage change over 2003-2013 estimated from a global mass budget
1185 approach. *Environmental Research Letters* 10(12), 124010, doi:10.1088/1748-
1186 9326/10/12/124010.
1187

1188 Dittmann, A., Schlosser, E., Masson-Delmotte, V., Powers, J.G., Manning, K.W., Werner,
1189 M., Fujita, K., 2016. Precipitation regime and stable isotopes at Dome Fuji, East Antarctica.
1190 *Atmospheric Chem. Phys.* 16, 6883–6900, doi:https://doi.org/10.5194/acp-16-6883-2016.
1191

1192 Donat-Magnin, M., Jourdain, M.C., Spence, P., Sommer, J.L., Gallée, H., Durand, G., 2017:
1193 Ice-Shelf Melt Response to Changing Winds and Glacier Dynamics in the Amundsen Sea
1194 Sector, Antarctica. *J. Geophys. Res. Oceans* 122, 10206–10224, doi:10.1002/2017JC013059.
1195

1196 Dufour, A., Charrondière, C., Zolina, O., 2019. Moisture transport in observations and
1197 reanalysis as a proxy for snow accumulation in East Antarctica. *Cryosphere* 13, 413-425.
1198

1199 Durand, G., Gagliardini, O., Favier, L., Zwinger, T., Le Meur, E., 2011. Impact of bedrock
1200 description on modeling ice sheet dynamics. *Geophys. Res. Lett.* 38, L20501,
1201 doi.org/10.1029/2011GL048892.
1202

1203 Dussaillant, I., Berthier, E., Brun, F., Masiokas, M., Hugonnet, R., Favier, V., Rabatel, A.,
1204 Pitte, P., Ruiz, L., 2018. Two decades of glacier mass loss along the Andes, *Nature*
1205 *Geoscience* 12, 802-808.

1206 Edwards, T.L., Brandon, M.A., Durand, G., Edwards, N.R., Golledge, N.R., Holden, P.H.,
1207 Nias, I.J., Payne, A.J., Ritz, C., Wernecke, A., 2019. Revisiting Antarctic ice loss due to
1208 marine ice-cliff instability. *Nature* 566, 58–64.
1209

1210 Enderlin, E.M., Howat, I.M., Jeong, S., Noh, M.-J., Van Angelen, J.H. and Van den Broeke,
1211 M.R., 2014. An improved mass budget for the Greenland ice sheet. *Geophysical Research*
1212 *Letters* 41, 866-872, 2013GL059010.
1213

1214 Eyring, V., Bony, S., Meehl, G.A., Senior, C.A., Stevens, B., Stouffer, R.J., Taylor, K.E.,
1215 2016. Overview of the Coupled Model Intercomparison Project Phase 6 (CMIP6)
1216 experimental design and organization. *Geosci. Model Dev.* 9, 1937-1958, doi:10.5194/gmd-
1217 9-1937-2016.
1218

1219 Favier, V., Agosta, C., Parouty, S., Durand, G., Delaygue, G., Gallée, H., Drouet, A.-S.,
1220 Trouvilliez, A., Krinner, G., 2013. An updated and quality controlled surface mass balance
1221 dataset for Antarctica. *Cryosphere* 7(2), 583-597, doi:10.5194/tc-7-583-2013.
1222

1223 Favier, V., Verfaillie, D., Berthier, B., Menegoz, M., Jomelli, V., Kay, J.E., Ducret, L.,
1224 Malbêteau, Y., Brunstein, D., Gallée, H., Park, Y.-H., Rinterknecht, V., 2016. Atmospheric
1225 drying as the main driver of dramatic glacier wastage in the southern Indian Ocean. *Sci. Rep.*
1226 6, 32396, doi:10.1038/srep32396.
1227

1228 Favier, V., Krinner, G., Amory, C., Gallée, H., Beaumet, J., Agosta, C., 2017. Antarctica-
1229 Regional Climate and Surface Mass Budget. *Curr. Clim. Change Rep.* 3, 303–315,
1230 doi:10.1007/s40641-017-0072-z.
1231

1232 Fettweis, X., 2018. The SMB Model Intercomparison (SMBMIP) over Greenland: first
1233 results. AGU Fall Meeting 2018, Washington, DC,
1234 <https://orbi.uliege.be/handle/2268/232923>.
1235

1236 Fettweis, X., Box J.E., Agosta, C., Amory, C., Kittel, C., Lang, C., van As, D., Machguth, H.,
1237 Gallée, H., 2017. Reconstructions of the 1900–2015 Greenland ice sheet surface mass
1238 balance using the regional climate MAR model. *The Cryosphere* 11(2), 1015-1033.
1239 doi:10.5194/tc-11-1015-2017.
1240

1241 Filament, T., Rémy, F., 2012. Dynamic thinning of Antarctic glaciers from along-track repeat
1242 radar altimetry. *J. Glaciol.* 58: 830–840. doi: 10.3189/2012JoG11J11.
1243

1244 Fischer, R., Nowicki, S., Kelley, M., Schmidt, G.A., 2014. A system of conservative
1245 regridding for ice-atmosphere coupling in a General Circulation Model (GCM), *Geosci.*
1246 *Model Dev.* 7, 883-907, doi:10.5194/gmd-7-883-2014.

1247
1248 Frezzotti, M., Urbini, S., Proposito, M., Sarchilli, C. Gandolfi, S., 2007. Spatial and
1249 temporal variability of surface mass balance near Talos Dome, East Antarctica. *J. Geophys.*
1250 *Res. Earth Surf.* 112, F02032, doi:10.1029/2006JF000638.

1251
1252 Fujita, S., Holmlund, P., Andersson, I., Brown, I., Enomoto, H., Fujii, Y., Fujita, K., Fukui,
1253 K., Furukawa, T., Hansson, M., Hara, K., Hoshina, Y., Igarashi, M., Iizuka, Y., Imura, S.,
1254 Ingvander, S., Karlin, T., Motoyama, H., Nakazawa, F., Oerter, H., Sjöberg, L.E., Sugiyama,
1255 S., Surdyk, S., Ström, J., Uemura, R., Wilhelms, F., 2011. Spatial and temporal variability of
1256 snow accumulation rate on the East Antarctic ice divide between Dome Fuji and EPICA
1257 DML. *The Cryosphere* 5, 1057–1081, doi:10.5194/tc-5-1057-2011.

1258
1259 Fyke, J.G., Sacks, W.J., Lipscomb, W.H., 2014a. A technique for generating consistent ice
1260 sheet initial conditions for coupled ice sheet/climate models. *Geosci. Model Dev.*, 7, 1183-
1261 1195, doi:10.5194/gmd-7-1183-2014, 2014.

1262
1263 Fyke, J.G., Vizcaino, M., Lipscomb, W.H., Price, S., 2014b. Future climate warming
1264 increases Greenland ice sheet surface mass balance variability. *Geophysical Research Letters*,
1265 41(2), 470-475.

1266
1267 Fyke, J.G., Vizcaino, M., Lipscomb, W.H., 2014c. The pattern of anthropogenic signal
1268 emergence in Greenland Ice Sheet surface mass balance. *Geophysical Research Letters*
1269 41(16), 6002-6008.

1270
1271 Fyke, J., Sergienko, O., Löfverström, M., Price, S., Lenaerts, J.T.M., 2018. An Overview of
1272 Interactions and Feedbacks Between Ice Sheets and the Earth System. *Rev. Geophys.* 56,
1273 361-408, doi:10.1029/2018RG000600.

1274
1275 Gao, C.C., Lu, Y., Zhang, Z.Z., Shi, H.L., Zhu, C.D., 2015. Ice sheet mass balance in
1276 Antarctica measured by GRACE and its uncertainty. *Chinese Journal of Geophysics-Chinese*
1277 *Edition* 58(3), 780-792.

1278
1279 Gao, C.C., Lu, Y., Shi, H.L., Zhang, Z.Z., Xu, C.Y. Tan, B., 2019a. Detection and analysis of
1280 ice sheet mass changes over 27 Antarctic drainage systems from GRACE RLO6 data.
1281 *Chinese Journal of Geophysics-Chinese Edition* 62(3), 864-882.

1282
1283 Gao, C.C., Lu, Y., Zhang, Z.Z. Shi, H.L., 2019b. A Joint Inversion Estimate of Antarctic Ice
1284 Sheet Mass Balance Using Multi-Geodetic Data Sets. *Remote Sens.* 11(6), 653,
1285 doi:10.3390/rs11060653.

1286
1287 Gardner, A. S., Moholdt, G., Cogley, J. G., Wouters, B., Arendt, A. A., Wahr, J., Berthier, E.,
1288 Hock, R., Pfeffer, W. T., Kaser, G., Ligtenberg, S. R. M., Bolch, T., Sharp, M. J., Hagen, J.
1289 O., van den Broeke, M. R., Paul, F., 2013. A reconciled estimate of glacier contributions to
1290 sea level rise: 2003 to 2009. *Science* 340, 852–857, doi:10.1126/science.1234532.

1291
1292 Gardner, A.S., Moholdt, G., Scambos, T., Fahnestock, M., Ligtenberg, S., Van den Broeke,
1293 M., Nilsson, J., 2018. Increased West Antarctic and unchanged East Antarctic ice discharge

1294 over the last 7 years. *The Cryosphere* 12, 521–547, doi:[https://doi.org/10.5194/tc-12-521-](https://doi.org/10.5194/tc-12-521-1295)
1295 2018.

1296

1297 Gillet-Chaulet, F., 2019. Assimilation of surface observations in a transient marine ice sheet
1298 model using an ensemble Kalman filter. *The Cryosphere Discuss*, [https://doi.org/10.5194/tc-](https://doi.org/10.5194/tc-2019-54)
1299 2019-54, in review.

1300

1301 Gillet-Chaulet, F., Gagliardini, O., Seddik, H., Nodet, M., Durand, G., Ritz, C., Zwinger, T.,
1302 Greve, R., Vaughan, D.G., 2012. Greenland ice sheet contribution to sea-level rise from a
1303 new-generation icesheet model. *Cryosphere* 6(6), 1561–76, doi:10.5194/tc-6-1561-2012.

1304

1305 Gillet-Chaulet, F., Durand, G., Gagliardini, O., Mosbeux, C., Mougnot, J., Rémy, F., Ritz,
1306 C., 2016. Assimilation of surface velocities acquired between 1996 and 2010 to constrain the
1307 form of the basal friction law under Pine Island Glacier. *Geophys. Res. Lett.* 43(19), 10311-
1308 10321, doi:10.1002/2016GL069937.

1309

1310 Gladstone, R.M., Payne, A.J., Cornford, S.L., 2012. Resolution requirements for grounding-
1311 line modelling: Sensitivity to basal drag and ice-shelf buttressing. *Ann Glaciol.* 53(60), 97–
1312 105. doi:10.3189/2012AoG60A148.

1313

1314 Goelzer, H., Nowicki, S., Edwards, T., Beckley, M., Abe-Ouchi, A., Aschwanden, A., Calov,
1315 R., Gagliardini, O., Gillet-Chaulet, F., Golledge, N.R., Gregory, J., Greve, R., Humbert, A.,
1316 Huybrechts, P., Kennedy, J H., Larour, E., Lipscomb, W.H., Le clec'h, S., Lee, V.,
1317 Morlighem, M., Pattyn, F., Payne, A.J., Rodehacke, C., Rückamp, M., Saito, F., Schlegel, N.,
1318 Seroussi, H., Shepherd, A., Sun, S., Van de Wal, R., Ziemen, F.A., 2018a: Design and results
1319 of the ice sheet model initialisation experiments initMIP-Greenland: an ISMIP6
1320 intercomparison. *The Cryosphere*, 12, 1433-1460, doi:10.5194/tc-12-1433-2018.

1321

1322 Goelzer, H., Nowicki, S., Edwards, T., Beckley, M., Abe-Ouchi, A., Aschwanden, A., Calov,
1323 R., Gagliardini, O., Gillet-Chaulet, F., Golledge, N.R., Gregory, J., Greve, R., Humbert, A.,
1324 Huybrechts, P., Kennedy, J.H., Larour, E., Lipscomb, W.H., Le clec'h, S., Lee, V.,
1325 Morlighem, M., Pattyn, F., Payne, A.J., Rodehacke, C., Rückamp, M., Saito, F., Schlegel, N.,
1326 Seroussi, H., Shepherd, A., Sun, S., Van de Wal, R., Ziemen, F.A., 2018b: Results of the ice
1327 sheet model initialisation experiments initMIP-Greenland: an ISMIP6 intercomparison,
1328 10.5281/zenodo.1173088.

1329

1330 Goldberg DN, Heimbach P, 2013. Parameter and state estimation with a time-dependent
1331 adjoint marine ice sheet model. *Cryosphere* 7(6),1659–78. doi:10.5194/tc-7-1659-2013.

1332

1333 Goldberg DN, Heimbach P, Joughin I, Smith B., 2015. Committed retreat of Smith, Pope,
1334 and Kohler Glaciers over the next 30 years inferred by transient model calibration.
1335 *Cryosphere* 9(6), 2429–46. doi:10.5194/tc-9-2429-2015.

1336

1337 Goldberg, D.N., Narayanan, S.H.K., Hascoet, L., Utke, J., 2016. An optimized treatment for
1338 algorithmic differentiation of an important glaciological fixed-point problem. *Geosci. Model*
1339 *Dev.* 9(5):1891–904, doi:10.5194/gmd-9-1891-2016.

1340

1341 Golledge, N.R., Kowalewski, D.E., Naish, T.R., Levy, R.H., Fogwill, C.J., Gasson, E.G.W.,
1342 2015. The multi-millennial Antarctic commitment to future sea-level rise. *Nature* 526, 421-
1343 425, <https://doi.org/10.1038/nature15706>.

1344
1345 Golledge, N.R., Keller, E.D., Gomez, N., Naughten, K.A., Bernales, J., Trusel, L.D., and
1346 Edwards, T.L., 2019. Global environmental consequences of twenty-first-century ice-sheet
1347 melt. *Nature* 566, 65-72, <https://doi.org/10.1038/s41586-019-0889-9>.
1348
1349 Gomez, N., Mitrovica, J.X., Huybers, P., Clark, P.U., 2010. Sea level as a stabilizing factor
1350 for marine-ice-sheet grounding lines. *Nature Geoscience* 3(12), 850-853.
1351
1352 Gomez, N., Pollard, D., Holland, D., 2015. Sea-level feedback lowers projections of future
1353 Antarctic Ice-Sheet mass loss. *Nature Communications*, 6: 8798.
1354
1355 Gomez, N., Latychev, K., Pollard, D., 2018. A coupled ice sheet-sea level model
1356 incorporating 3D Earth structure: Variations in Antarctica during the last deglacial retreat.
1357 *Journal of Climate* 31(10), 4041-4054.
1358
1359 Gorodetskaya, I.V., Tsukernik, M., Claes, K., Ralph, M.F., Neff, W.D., Van Lipzig, N.P.M.,
1360 2014. The role of atmospheric rivers in anomalous snow accumulation in East Antarctica.
1361 *Geophys. Res. Lett.* 41, 6199–6206, doi:10.1002/2014GL060881.
1362
1363 Gorodetskaya, I.V., Kneifel, S., Maahn, M., Thiery, W., Schween, J.H., Mangold, A.,
1364 Crewell, S., Van Lipzig, N.P.M., 2015. Cloud and precipitation properties from ground-based
1365 remote-sensing instruments in East Antarctica. *The Cryosphere* 9, 285–304, doi:10.5194/tc-9-
1366 285-2015.
1367
1368 Grazioli, J., Genthon, C., Boudevillain, B., Duran-Alarcon, C., Del Guasta, M., Madeleine,
1369 J.-B., Berne, A., 2017a. Measurements of precipitation in Dumont d’Urville, Adélie
1370 Land, East Antarctica. *The Cryosphere* 11, 1797–1811, doi:10.5194/tc-11-1797-2017.
1371
1372 Grazioli, J., Madeleine, J.-B., Gallée, H., Forbes, R.M., Genthon, C., Krinner, G., Berne, A.,
1373 2017b. Katabatic winds diminish precipitation contribution to the Antarctic ice mass balance.
1374 *Proc. Natl. Acad. Sci.* 114, 10858–10863, doi:10.1073/pnas.1707633114.
1375
1376 Groh, A., Ewert, H., Fritsche, M., Rulke, A., Rosenau, R., Scheinert, M., Dietrich, R., 2014a.
1377 Assessing the Current Evolution of the Greenland Ice Sheet by Means of Satellite and
1378 Ground-Based Observations. *Surveys in Geophysics* 35(6), 1459-1480.
1379
1380 Groh, A., Ewert, H., Rosenau, R., Fagiolini, E., Gruber, C., Floricioiu, D., Jaber, W.A.,
1381 Linow, S., Flechtner, F., Eineder, M., Dierking, W. and Dietrich, R., 2014b. Mass, Volume
1382 and Velocity of the Antarctic Ice Sheet: Present-Day Changes and Error Effects. *Surveys in*
1383 *Geophysics* 35(6), 1481-1505.
1384
1385 Gunter, B.C., Didova, O., Riva, R.E.M., Ligtenberg, S.R.M., Lanaerts, J.T.M., King, M., van
1386 den Broeke, M.R., Urban, T., 2014. Empirical estimation of present-day Antarctic glacial
1387 isostatic adjustment and ice mass change. *The Cryosphere* 8(2), 743-760.
1388
1389 Hanna, E., Navarro, F.J., Pattyn, F., Domingues, C.M., Fettweis, X., Ivins, E.R., Nicholls,
1390 R.J., Ritz, C., Smith, B., Tulaczyk, S., Whitehouse, P.L., Zwally, H.J., 2013. Ice-sheet mass
1391 balance and climate change. *Nature* 498 (7452), 51-59.
1392

1393 Hanna, E., Fettweis, X., Mernild, S.H., Cappelen, J., Ribergaard, M.H., Shuman, C.A.,
1394 Steffen, K., Wood, L., Mote, T.L., 2014. Atmospheric and oceanic climate forcing of the
1395 exceptional Greenland ice sheet surface melt in summer 2012. *International Journal of*
1396 *Climatology* 34, 1022-1037.

1397
1398 Hanna, E., Cropper, T.R., Hall, R.J., Cappelen, J., 2016. Greenland Blocking Index 1851-
1399 2015: a regional climate change signal. *International Journal of Climatology* 36, 4847-4861.

1400
1401 Hanna, E., Fettweis, X. and Hall R.J., 2018: Brief communication: Recent changes in
1402 summer Greenland blocking captured by none of the CMIP5 models. *The Cryosphere* 12(10),
1403 3287-3292.

1404
1405 Harig, C., Simons, F.J., 2015. Accelerated West Antarctic ice mass loss continues to outpace
1406 East Antarctic gains. *Earth and Planetary Science Letters* 415, 134-141.

1407
1408 Hermann, M., Box, J.E., Fausto, R.S., Colgan, W.T., Langen, P.L., Mottram, R., Wuite, J.,
1409 Noël, B., Van den Broeke, M.R., Van As, D., 2018. Application of PROMICE Q-Transect in
1410 Situ Accumulation and Ablation Measurements (2000-2017) to Constrain Mass Balance at
1411 the Southern Tip of the Greenland Ice Sheet. *J. Geophys. Res.-Earth* 123(6), 1235-1256.

1412
1413 Hock, R., Bliss, A., Marzeion, B., Giesen, R., Hirabayashi, Y., Huss, M., Radić, V., Slangen,
1414 A., 2019. GlacierMIP – A model intercomparison of global-scale glacier mass-balance
1415 models and projections. *Journal of Glaciology* 65, 453-467, doi:10.1017/jog.2019.22.

1416
1417 Hubbard, B., Luckman, A., Ashmore, D.W., Bevan, S., Kulesa, B., Kuipers Munneke, P.,
1418 Philippe, M., Jansen, D., Booth, A., Sevestre, H., Tison, J.-L., O’Leary, M., Rutt, I., 2016.
1419 Massive subsurface ice formed by refreezing of ice-shelf melt ponds. *Nat. Commun.* 7,
1420 11897, doi:10.1038/ncomms11897.

1421
1422 Hurkmans, R., Bamber, J.L., Davis, C.H., Joughin, I.R., Khvorostovsky, K.S., Smith, B.S.,
1423 Schoen, N., 2014. Time-evolving mass loss of the Greenland Ice Sheet from satellite
1424 altimetry. *Cryosphere* 8(5), 1725-1740.

1425
1426 Huss, M., 2013. Density assumptions for converting geodetic glacier volume change to mass
1427 change. *The Cryosphere* 7, 877–887, doi:10.5194/tc-7-877-2013.

1428
1429 Huss, M., Farinotti, D., 2012. Distributed ice thickness and volume of all glaciers around the
1430 globe. *Journal of Geophysical Research* 117, F04010, doi:10.1029/2012JF002523.

1431
1432 Huss, M., Hock, R., 2015. A new model for global glacier change and sea-level rise.
1433 *Frontiers in Earth Science* 3, 54, doi:10.3389/feart.2015.00054.

1434
1435 Huss, M., Jouvett, G., Farinotti, D., Bauder, A., 2010. Future high-mountain hydrology: a new
1436 parameterization of glacier retreat. *Hydrology and Earth System Sciences* 14, 815–829,
1437 doi:10.5194/hess-14-815-2010.

1438
1439 IPCC, 2013. *Climate Change 2013: The Physical Science Basis. Contribution of Working*
1440 *Group I to the Fifth Assessment Report of the Intergovernmental Panel on Climate Change*,
1441 edited by: Stocker, T. F., Qin, D., Plattner, G.-K., Tignor, M., Allen, S. K., Boschung, J.,

1442 Nauels, A., Xia, Y., Bex, V., and Midgley, P. M., Cambridge University Press, Cambridge,
1443 United Kingdom and New York, NY, USA.
1444

1445 Ivins, E.R., James, T.S., Wahr, J., Schrama, E.J.O., Landerer, F.W., Simon, K.M., 2013.
1446 Antarctic Contribution to Sea-Level Rise Observed by GRACE with Improved GIA
1447 Correction. *Journal of Geophysical Research: Solid Earth* 118(6), 3126-3141.
1448

1449 Jacob, T., Wahr, J., Pfeffer, W.T., Swenson, S., 2012. Recent contributions of glaciers and ice
1450 caps to sea level rise. *Nature* 482(7386), 514–518. doi:10.1038/nature10847.
1451

1452 Jamieson, S.S.R., Vieli, A., Livingstone, S.J., Ó Cofaigh, C., Stokes, C., Hillenbrand, C.-D.,
1453 Dowdeswell, J.A. 2012. Ice-stream stability on a reverse bed slope. *Nature Geoscience* 5,
1454 799-802.
1455

1456 Jenkins, A., Dutrieux, P., Jacobs, S.S., McPhail, S.D., Perrett, J.R., Webb, A.T., White, D.,
1457 2010. Observations beneath Pine Island Glacier in West Antarctica and implications for its
1458 retreat. *Nat. Geosci.* 3, 468–472, doi:10.1038/ngeo890.
1459

1460 Jin, S., Abd-Elbaky, M., Feng, G., 2016. Accelerated ice-sheet mass loss in Antarctica from
1461 18-year satellite laser ranging measurements. *Annals of Geophysics* 59(1), doi: 10.4401/ag-
1462 6782.
1463

1464 Jones, J.M., Gille, S.T., Goosse, H., Abram, N.J., Canziani, P.O., Charman, D.J., Clem, K.R.,
1465 Crosta, X., de Lavergne, C., Eisenman, I., England, M.H., Fogt, R.L., Frankcombe, L.M.,
1466 Marshall, G.J., Masson-Delmotte, V., Morrison, A.K., Orsi, A.J., Raphael, M.N., Renwick
1467 J.A., Schneider, D.P., Simpkins, G.R., Steig, E.J., Stenni, B., Swingedouw, D., Vance, T.R.,
1468 2016. Assessing recent trends in high-latitude Southern Hemisphere surface climate. *Nat.*
1469 *Clim. Change* 6, 917–926, doi:10.1038/nclimate3103.
1470

1471 Joughin, I., Smith, B.E., Medley, B., 2014. Marine ice sheet collapse potentially under way
1472 for the Thwaites Glacier Basin, West Antarctica. *Science* 344, 735–738.
1473

1474 Khan, S.A., Sasgen, I., Bevis, M., van Dam, T., Bamber, J.L., Wahr, J., Willis, M., Kjaer,
1475 K.H., Wouters, B., Helm, V., Csatho, B., Fleming, K., Bjork, A.A., Aschwanden, A.,
1476 Knudsen, P., Munneke, P.K., 2016. Geodetic measurements reveal similarities between post-
1477 Last Glacial Maximum and present-day mass loss from the Greenland ice sheet. *Science*
1478 *Advances* 2(9), doi:10.1126/sciadv.1600931.
1479

1480 Khvorostovsky, K. S., 2012. Merging and analysis of elevation time series over Greenland
1481 Ice Sheet from satellite radar altimetry, *IEEE Trans. Geosci. Remote Sens.* 50: 23–36,
1482 doi:10.1109/TGRS.2011.2160071.
1483

1484 Kimura, S., Jenkins, A., Dutrieux, P., Forryan, A., Garabato, A.C.N., Firing, Y., 2016. Ocean
1485 mixing beneath Pine Island Glacier ice shelf, West Antarctica. *J. Geophys. Res. Oceans* 121,
1486 8496–8510, doi:10.1002/2016JC012149.
1487

1488 King, M.A., Bingham, R.J., Moore, P., Whitehouse, P.L., Bentley, M.J., Milne, G.A., 2012.
1489 Lower satellite-gravimetry estimates of Antarctic sea-level contribution. *Nature* 491(7425),
1490 586-589.
1491

1492 Kingslake, J., Ng, F., Sole, A., 2015. Modelling channelized surface drainage of supraglacial
1493 lakes. *J. Glaciol.* 61, 185–199.

1494

1495 Kingslake, J., Ely, J.C., Das, I., Bell, R.E., 2017. Widespread movement of meltwater onto
1496 and across Antarctic ice shelves. *Nature* 544, 349–352, doi:10.1038/nature22049.

1497

1498 Kingslake, J., Scherer, R.P., Albrecht, T., Coenen, J., Powell, R.D., Reese, R., Stansell, N.D.,
1499 Tulaczyk, S., Wearing, M.G., Whitehouse, P.L., 2018. Extensive retreat and re-advance of
1500 the West Antarctic Ice Sheet during the Holocene. *Nature*, 558(7710): 430-434.

1501

1502 Kjeldsen, K.K., Korsgaard, N.J., Bjørk, A.A., Khan, S.A., Box, J.E., Funder, S., Larsen,
1503 N.K., Bamber, J.L., Colgan, W., Van den Broeke, M., Siggaard-Andersen, M.-L., Nuth, C.,
1504 Schomacker, A., Andresen, C.S., Willerslev, E., Kjaer, K.H., 2015. Spatial and temporal
1505 distribution of mass loss from the Greenland Ice Sheet since AD 1900. *Nature* 528, 396-400.

1506

1507 Koenig, L.S., Ivanoff, A., Alexander, P.M., MacGregor, J.A., Fettweis, X., Panzer, B., Paden,
1508 J. D., Forster, R.R., Das, I., McConnell, J.R., Tedesco, M., Leuschen, C., and Gogineni, P.,
1509 2016. Annual Greenland accumulation rates (2009–2012) from airborne snow radar, *The*
1510 *Cryosphere* 10, 1739-1752, <https://doi.org/10.5194/tc-10-1739-2016>

1511

1512 Konrad, H., Sasgen, I., Pollard, D., Klemann, V., 2015. Potential of the solid-Earth response
1513 for limiting long-term West Antarctic Ice Sheet retreat in a warming climate. *Earth Planet.*
1514 *Sci. Lett.* 432, 254-264.

1515

1516 Krinner, G., Langeron, C., Ménégoz, M., Agosta, C., Brutel-Vuilmet, C., 2014. Oceanic
1517 Forcing of Antarctic Climate Change: A Study Using a Stretched-Grid Atmospheric General
1518 Circulation Model. *J. Clim.* 27, 5786–5800, doi:10.1175/JCLI-D-13-00367.1.

1519

1520 Krinner, G., Beaumet, J., Favier, V., Déqué, M., Brutel-Vuilmet, C., 2019. Empirical run -
1521 time bias correction for Antarctic regional climate projections with a stretched-grid AGCM.
1522 *Journal of Advances in Modeling Earth Systems* 11, 64–82.

1523

1524 Kronenberg, M., Barandun, M., Hoelzle, M., Huss, M., Farinotti, D., Azisov, E., Usubaliev,
1525 R., Gafurov, A., Petrakov, D., Kääh, A., 2016. Mass-balance reconstruction for Glacier No.
1526 354, Tien Shan, from 2003 to 2014. *Annals of Glaciology* 57(71), 92–102.
1527 doi:10.3189/2016AoG71A032.

1528

1529 Kuipers Munneke, P., Luckman, A.J., Bevan, S.L., Smeets, C.J.P.P., Gilbert, E., Van den
1530 Broeke, M.R., Wang, W., Zender, C., Hubbard, B., Ashmore, D., Orr, A., King, J.C.,
1531 Kulesa, B., 2018. Intense winter surface melt on an Antarctic ice shelf. *Geophys. Res. Lett.*
1532 45 (15), 7615-7623, <https://doi.org/10.1029/2018GL077899>.

1533

1534 Larour, E., Seroussi, H., Adhikari, Z., Ivins, E., Caron, L., Morlighem, M., Schlegel, N.,
1535 2019: Slowdown in Antarctic mass loss from solid Earth and sea-level feedbacks. *Science*
1536 364 (6444), 10.1126/science.aav7908.

1537

1538 Leclercq, P.W., Oerlemans, J., Cogley, J. G., 2011. Estimating the glacier contribution to sea-
1539 level rise for the period 1800–2005. *Surv. Geophys.* 32, 519–535. doi:10.1007/s10712-011-
1540 9121-7.

1541

1542 Leclercq, P.W., Weidick, A., Paul, F., Bolch, T., Citterio, M., Oerlemans, J., 2012. Brief
1543 communication “Historical glacier length changes in West Greenland”. *The Cryosphere* 6,
1544 1339–1343, doi:10.5194/tc-6-1339-2012.

1545

1546 Leclercq, P.W., Oerlemans, J., Basagic, H.J., Bushueva, I., Cook, A.J., Le Bris, R., 2014. A
1547 data set of worldwide glacier length fluctuations. *The Cryosphere* 8, 659–672.
1548 doi:10.5194/tc-8-659-2014.

1549

1550 Lenaerts, J.T.M., van Den Broeke, M.R., Scarchilli, C., Agosta, C., 2012. Impact of model
1551 resolution on simulated wind, drifting snow and surface mass balance in Terre Adélie, East
1552 Antarctica. *J. Glaciol.* 58(211), 821–829. doi:10.3189/2012JoG12J020.

1553

1554 Lenaerts, J.T.M., Le Bars, D., Kampenhout, L., Vizcaino, M., Enderlin, E.M., van den
1555 Broeke, M.R., 2015. Representing Greenland ice sheet freshwater fluxes in climate models,
1556 *Geophys. Res. Lett.* 42, 6373– 6381, doi:10.1002/2015GL064738.

1557

1558 Lenaerts J.T.M., Vizcaino M., Fyke J., van Kampenhout L., van den Broeke M.R., 2016.
1559 Present-day and future Antarctic ice sheet climate and surface mass balance in the
1560 Community Earth System Model. *Climate Dynamics* 47(5-6), 1367–1381.
1561 doi:10.1007/s00382-015-2907-4.

1562

1563 Lenaerts, J.T.M., Lhermitte, S., Drews, R., Ligtenberg, S.R.M., Berger, S., Helm, V., Smeets,
1564 C.J.P.P., van den Broeke, M.R., van de Berg, W.J., van Meijgaard, E., Eijkelboom, M., Elsen,
1565 O., Pattyn, F., 2017. Meltwater produced by wind-albedo interaction stored in an East
1566 Antarctic ice shelf. *Nature Climate Change* 7(1), 58–62. doi:10.1038/nclimate3180.

1567

1568 Lenaerts, J., Ligtenberg, S.R.M., Medley, B., van de Berg, W.J., Konrad, H., Nicolas, J.P.,
1569 van Wessem, J.M., Trusel, L.D., Mulvaney, R., Tuckwell, R.J., Hogg, A.E., Thomas, E.R.,
1570 2018. Climate and surface mass balance of coastal West Antarctica resolved by regional
1571 climate modelling. *Ann. Glaciol.* 59(76), 29–41, doi:10.1017/aog.2017.42.

1572

1573 Levermann, A., Winckermann, R., Nowicki, S., Fastook, J. L., Frieler, K., Greve, R., Hellmer,
1574 H.H., Martin, M.A., Meinshausen, M., Mengel, M., Payne, A.J., Pollard, D., Sato, T.,
1575 Timmermann, R., Wang, W.L., Bindschadler, R.A., 2014. Projecting Antarctic ice discharge
1576 using response functions from SeaRISE ice-sheet models. *Earth System Dynamics* 5, 271-
1577 293, <https://doi.org/10.5194/esd-5-271-2014>.

1578

1579 Lewis, G., Osterberg, E., Hawley, R., Whitmore, B., Marshall, H.P., Box, J., 2017. Regional
1580 Greenland accumulation variability from Operation IceBridge airborne accumulation radar.
1581 *Cryosphere* 11(2), 773-788, doi:10.5194/tc-11-773-2017.

1582

1583 Li, J., Zwally, H.J., 2015. Response times of ice-sheet surface heights to changes in the rate
1584 of Antarctic firn compaction caused by accumulation and temperature variations. *J. Glaciol.*,
1585 61, 1037–1047, doi: 10.3189/2015JoG14J082.

1586

1587 Li, F., Yuan, L.X., Zhang, S.K., Yang, Y.D., E, D.C., Hao, W.F., 2016. Mass change of the
1588 Antarctic ice sheet derived from ICESat laser altimetry. *Chinese Journal of Geophysics-
1589 Chinese Edition* 59(1), 93-100.

1590

1591 Libois, Q., Picard, G., Arnaud, L., Morin, S., Brun, E., 2014. Modeling the impact of snow
1592 drift on the decameter-scale variability of snow properties on the Antarctic Plateau. *J.*
1593 *Geophys. Res. Atmospheres* 119, 11,662–11,681, doi:10.1002/2014JD022361.

1594 Lipscomb, W., Fyke, J.G., Vizcaino, M., Sacks, W., Wolfe, J., Vertenstein, M., Craig, A.,
1595 Kluzek, E., Lawrence D., 2013. Implementation and Initial Evaluation of the Glimmer
1596 Community Ice Sheet Model in the Community Earth System Model. *Journal of Climate*
1597 26(19), 7352-7371.

1598
1599 Lucas-Picher, P., Wulff-Nielsen, M., Christensen, J.H., Adalgeirsdóttir, G., Mottram, R.H.,
1600 Simonsen, S.B., 2012. Very high resolution regional climate model simulations over
1601 Greenland: Identifying added value. *J. Geophys. Res.* 117, D02108.
1602 doi:10.1029/2011JD016267.

1603 Luthcke, S.B., Arendt, A.A., Rowlands, D.D., Mccarthy, J.J., Larsen C.F., 2008. Recent
1604 glacier mass changes in the Gulf of Alaska region from GRACE mascon solutions. *J.*
1605 *Glaciol.*, 54(188), 767-777.

1606
1607 MacAyeal, D.R., 1992. The basal stress distribution of Ice Stream E, Antarctica, inferred by
1608 control methods. *J. Geophys. Res.* 97(B1), 595-603, doi:10.1029/91JB02454.

1609
1610 Machguth, H., Thomsen, H.H., Weidick, A., Ahlstrøm, A.P., Abermann, J., Andersen, M.L.,
1611 Andersen, S.B., Bjørk, A.A., Box, J.E., Braithwaite, R.J., Bøggild, C.E., Citterio, M.,
1612 Clement, P., Colgan, W., Fausto, R.S., Gleie, K., Gubler, S., Hasholt, B., Hynek, B.,
1613 Knudsen, N.T., Larsen, S.H., Mernild, S.H., Oerlemans, J., Oerter, H., Olesen, O.B., Smeets,
1614 C.J.P.P., Steffen, K., Stober, M., Sugiyama, S., van As, D., van den Broeke, M.R., van de
1615 Wal, R.S.W., 2016. Greenland surface mass-balance observations from the ice-sheet ablation
1616 area and local glaciers. *J Glaciol.* 62(235), 861-887, doi:10.1017/jog.2016.75.

1617
1618 Martín-Español, A., Zammit-Mangion, A., Clarke, P.J., Flament, T., Helm, V., King, M.A.,
1619 Luthcke, S.B., Petrie, E., Remy, F., Schon, N., Wouters, B., Bamber, J.L., 2016. Spatial and
1620 temporal Antarctic Ice Sheet mass trends, glacio-isostatic adjustment, and surface processes
1621 from a joint inversion of satellite altimeter, gravity, and GPS data. *J. Geophys. Res.: Earth*
1622 *Surface* 121(2), 182-200.

1623
1624 Martín-Español, A., Bamber, J.L., Zammit-Mangion, A., 2017. Constraining the mass
1625 balance of East Antarctica. *Geophys. Res. Lett.* 44, 4168-4175, doi:10.1002/2017GL072937.

1626
1627 Marzeion, B., Jarosch, A. H., Hofer, M., 2012. Past and future sea-level change from the
1628 surface mass balance of glaciers. *The Cryosphere* 6, 1295–1322, doi:10.5194/tc-6-1295-2012.

1629
1630 Marzeion, B., Cogley, J.G., Richter, K., Parkes, D., 2014a. Attribution of global glacier mass
1631 loss to anthropogenic and natural causes. *Science* 345(6199), 919–921.
1632 doi:10.1126/science.1254702.

1633
1634 Marzeion, B., Jarosch, A.H., Gregory, J.M., 2014b. Feedbacks and mechanisms affecting the
1635 global sensitivity of glaciers to climate change. *The Cryosphere* 8, 59–71, doi: 10.5194/tc-8-
1636 59-2014.

1637

1638 Marzeion, B., Leclercq, P.W., Cogley, J.G., Jarosch, A.H., 2015. Brief communication:
1639 global reconstructions of glacier mass change during the 20th century are consistent. *The*
1640 *Cryosphere* 9, 2399–2404, doi:10.5194/tc-9-2399-2015.

1641
1642 Marzeion, B., Champollion, N., Haeberli, W., Langley, K., Leclercq, P., Paul, F., 2017.
1643 Observation-based estimates of global glacier mass change and its contribution to sea-level
1644 change. *Surv. Geophys.* 38, 105–30, doi:10.1007/s10712-016-9394-y.

1645
1646 Marzeion, B., Kaser, G., Maussion, F., Champollion, N., 2018. Limited influence of climate
1647 change mitigation on short-term glacier mass loss. *Nature Climate Change* 8, 305–308, doi:
1648 10.1038/s41558-018-0093-1.

1649
1650 Massom, R.A., Pook, M.J., Comiso, J.C., Adams, N., Turner, J., Lachlan-Cope, T., Gibson,
1651 T.T., 2004. Precipitation over the interior East Antarctic Ice Sheet related to midlatitude
1652 blocking-high activity. *J. Clim.* 17, 1914–1928.

1653
1654 McMillan, M., Shepherd, A., Sundal, A., Briggs, K., Muir, A., Ridout, A., Hogg, A.,
1655 Wingham, D., 2014. Increased ice losses from Antarctica detected by CryoSat-2. *Geophys.*
1656 *Res. Lett.* 41(11), 3899-3905.

1657
1658 McMillan, M., Leeson, A., Shepherd, A., Briggs, K., Armitage, T.W.K., Hogg, A., Kuipers
1659 Munneke, P., van den Broeke, M., Noël, B., van de Berg, W.J., Ligtenberg, S., Horwath, M.,
1660 Groh, A., Muir, A., Gilbert, L., 2016. A high-resolution record of Greenland mass balance.
1661 *Geophys. Res. Lett.* 43, 7002-7010.

1662
1663 Medley, B., Thomas, E.R., 2019. Increased snowfall over the Antarctic Ice Sheet mitigated
1664 twentieth-century sea-level rise. *Nature Climate Change* 9, 34-39.

1665
1666 Medley, B., Joughin, I., Das, S.B., Steig, E.J., Conway, H., Gogineni, S., Criscitiello, A.S.,
1667 McConnell, J.R., Smith, B.E., van den Broeke, M.R., Lenaerts, J.T.M., Bromwich, D.H.,
1668 Nicolas J.P., 2013. Airborne-radar and ice-core observations of annual snow accumulation
1669 over Thwaites Glacier, West Antarctica confirm the spatiotemporal variability of global and
1670 regional atmospheric models. *Geophys. Res. Lett.* 40, 3649–3654, doi:10.1002/grl.50706.

1671
1672 Medley, B., Ligtenberg, S.R.M., Joughin, I., van den Broeke, M.R., Gogineni, S. and
1673 Nowicki, S., 2015. Antarctic firn compaction rates from repeat-track airborne radar data: I.
1674 *Methods. Ann. Glaciol.* 56, 155–166, doi:10.3189/2015AoG70A203.

1675
1676 Melkonian, A.K., Willis, M.J., Pritchard M.E., Stewart A.J., 2016. Recent changes in glacier
1677 velocities and thinning at Novaya Zemlya. *Remote Sensing of the Environment* 174, 244–
1678 257, doi:10.1016/j.rse.2015.11.001.

1679
1680 Memin, A., Flament, T., Remy, F., Llubes, M., 2014. Snow- and ice-height change in
1681 Antarctica from satellite gravimetry and altimetry data. *Earth Planet. Sci. Lett.* 404, 344-353.

1682
1683 Moholdt, G., Nuth, C., Hagen, J.O., Kohler, J., 2010. Recent elevation changes of Svalbard
1684 glaciers derived from ICESat laser altimetry. *Remote Sens. Environ.*, 114(11), 2756-2767,
1685 doi:10.1016/j.rse.2010.06.008.

1686

- 1687 Montgomery, L., Koenig, L., and Alexander, P., 2018. The SUMup dataset: compiled
1688 measurements of surface mass balance components over ice sheets and sea ice with analysis
1689 over Greenland. *Earth Syst. Sci. Data* 10, 1959-1985.
- 1690 Moon, T., Joughin, I., Smith, B., Howat, I., 2012. 21st-century evolution of Greenland outlet
1691 glacier velocities. *Science* 336(6081), 576-578.
- 1692
1693 Mordret, A., 2018. Uncovering the Iceland hot spot track beneath Greenland. *J. Geophys.*
1694 *Res.-Solid Earth*, 123(6), 4922-4941.
- 1695
1696 Morlighem, M., Rignot, E., Seroussi, H., Larour, E., Ben Dhia, H., Aubry, D., 2010. Spatial
1697 patterns of basal drag inferred using control methods from a full-Stokes and simpler models
1698 for Pine Island Glacier, West Antarctica. *Geophys Res Lett.* 37(14), 1–6,
1699 doi:10.1029/2010GL043853.
- 1700
1701 Morlighem, M., Seroussi, H., Larour, E., Rignot, E., 2013. Inversion of basal friction in
1702 Antarctica using exact and incomplete adjoints of a higher-order model. *J. Geophys. Res.*
1703 *Earth Surf.* 118 (3), 1746–53, doi:10.1002/jgrf.20125.
- 1704
1705 Mouginit, J., Rignot, E., Bjørk, A., van den Broeke, M., Millan, R., Morlighem, M., Noël,
1706 B., Scheuchl, B., Wood, M., 2019. Forty-six years of Greenland Ice Sheet mass balance:
1707 1972 to 2018. *PNAS* 116 (19), 9239-9244, doi.org/10.1073/pnas.1904242116.
- 1708
1709 Nias, I. J., Cornford, S.L., Payne, A.J., 2016. Contrasting the modelled sensitivity of the
1710 Amundsen Sea embayment ice streams. *J. Glaciol.* 62, 552–562.
- 1711
1712 Nicholls, K.W., Abrahamsen, E.P., Buck, J.J.H., Dodd, P.A., Goldblatt, C., Griffiths, G.,
1713 Heywood, K.J., Hughes, N.E., Kaletzký, A., Lane-Serff, G.F., McPhail, S.D., Millard, N.W.,
1714 Oliver, K.I.C.; Perrett, J.; Price, M.R.; Pudsey, C.J.; Saw, K.; Stansfield, K.; Stott, M.J.;
1715 Wadhams, P., Webb, A.T., Wilkinson, J.P., 2006. Measurements beneath an Antarctic ice
1716 shelf using an autonomous underwater vehicle. *Geophys. Res. Lett.* 33, L08612,
1717 doi:10.1029/2006GL025998.
- 1718
1719 Nick, F.M., Vieli, A., Andersen, M.L., Joughin, I., Payne, A., Edwards, T.L., Pattyn, F., Van
1720 De Wal, R.S.W., 2013. Future sea-level rise from Greenland’s main outlet glaciers in a
1721 warming climate. *Nature.* 497(7448), 235–238, doi:10.1038/nature12068.
- 1722
1723 Nicolas, J.P., Vogelmann, A.M., Scott, R.C., Wilson, A.B., Cadeddu, M.P., Bromwich, D.H.,
1724 Verlinde, J., Lubin, D., Russell, L.M., Jenkinson, C., Powers, H.H., Ryczek, M., Stone, G.,
1725 Wille, J.D., 2017. January 2016 extensive summer melt in West Antarctica favoured by
1726 strong El Niño. *Nat. Commun.* 8, 15799, doi:10.1038/ncomms15799.
- 1727
1728 Nield, G.A., Barletta, V.R., Bordoni, A., King, M.A., Whitehouse, P.L., Clarke, P.J.,
1729 Domack, E., Scambos, T.A., Berthier, E., 2014. Rapid bedrock uplift in the Antarctic
1730 Peninsula explained by viscoelastic response to recent ice unloading. *Earth Planet. Sci. Lett.*
1731 397, 32-41.
- 1732
1733 Nilsson, J., Gardner, A., Sørensen, L.S., Forsberg, R., 2016. Improved retrieval of land ice
1734 topography from CryoSat-2 data and its impact for volume-change estimation of the
1735 Greenland Ice Sheet. *The Cryosphere* 10, 2953-2969.

1736
1737 Noël, B., van de Berg, W. J., van Wessem, J. M., van Meijgaard, E., van As, D., Lenaerts, J.
1738 T. M., Lhermitte, S., Kuipers Munneke, P., Smeets, C. J. P. P., van Uft, L. H., van de Wal,
1739 R. S. W., van den Broeke, M. R., 2018a. Modelling the climate and surface mass balance of
1740 polar ice sheets using RACMO2 – Part 1: Greenland (1958–2016). *The Cryosphere* 12, 811-
1741 831.
1742
1743 Noël, B., van de Berg, W.J., Lhermitte, S., Wouters, B., Schaffer, N., and van den Broeke,
1744 M.R., 2018b. Six decades of glacial mass loss in the Canadian Arctic Archipelago. *J.*
1745 *Geophys. Res.: Earth Surface* 123, 1430–1449. doi: 10.1029/2017JF004304.
1746
1747 Nowicki, S. M. J., Payne, A., Larour, E., Seroussi, H., Goelzer, H., Lipscomb, W., Gregory,
1748 J., Abe-Ouchi, A., Shepherd, A., 2016. Ice Sheet Model Intercomparison Project (ISMIP6)
1749 contribution to CMIP6, *Geosci. Model Dev.* 9, 4521-4545, doi:10.5194/gmd-9-4521-2016.
1750
1751 Palerme, C., J. E. Kay, C. Genthon, T. L’Ecuyer, N. B. Wood, C. Claud, 2014. How much
1752 snow falls on the Antarctic ice sheet? *The Cryosphere* 8, 1577–1587, doi:10.5194/tc-8-1577-
1753 2014.
1754
1755 Palerme, C., C. Genthon, C. Claud, J. E. Kay, N. B. Wood, T. L’Ecuyer, 2017. Evaluation of
1756 current and projected Antarctic precipitation in CMIP5 models. *Clim. Dyn.* 48, 225–239,
1757 doi:10.1007/s00382-016-3071-1.
1758
1759 Parkes, D., Marzeion, B., 2018. Twentieth-century contribution to sea-level rise from
1760 uncharted glaciers. *Nature* 563, 551-554, doi:10.1038/s41586-018-0687-9.
1761
1762 Pattyn, F., Schoof, C., Perichon, L, Hindmarsh, R.C.A., Bueler, E., De Fleurian, B., Durand,
1763 G., Gagliardini, O., Gladstone, R., Goldberg, D., Gudmundsson, G.H., Huybrechts, P., Lee,
1764 V., Nick, F.M., Payne, A.J., Pollard, D., Rybak, O., Saito, F., Vieli, A., 2012. Results of the
1765 marine ice sheet model intercomparison project, MISMIP. *Cryosphere* 6(3), 573–88,
1766 doi:10.5194/tc-6-573-2012.
1767
1768 Pattyn, F., Perichon, L., Durand, G., Favier, L., Gagliardini, O., Hindmarsh, R.C.A., Zwinger,
1769 T., Albrecht, T., Cornford, S., Docquier, D., F’urst, J.J., Goldberg, D., Gudmundsson, G.H.,
1770 Humbert, A., Hütten, M., Huybrechts, P., Jouvét, G., Kleiner, T., Larour, E., Martin, D.,
1771 Morlighem, M., Payne, A.J., Pollard, D., Rückamp, M., Rybak, O., Seroussi, H., Thoma, M.,
1772 Wilkens, N., 2013. Grounding-line migration in plan-view marine ice-sheet models: Results
1773 of the ice2sea MISMIP3d intercomparison. *J Glaciol.* 59(215), 410–22,
1774 doi:10.3189/2013JoG12J129.
1775
1776 Pattyn, F., Favier, L., Sun, S., Durand, G., 2017. Progress in Numerical Modeling of
1777 Antarctic Ice-Sheet Dynamics. *Curr. Clim. Change Rep.* 3, 174–184, doi:10.1007/s40641-
1778 017-0069-7.
1779
1780 Pattyn, F., Ritz, C., Hanna, E., Asay-Davis, X., DeConto, R., Durand, G., Favier, L.,
1781 Fettweis, X., Goelzer, H., Golledge, N.R., Munneke, P.K., Lenaerts, J.T.M., Nowicki, S.,
1782 Payne, A.J., Robinson, A., Seroussi, H., Trusel, L.D., van den Broeke, M., 2018. The
1783 Greenland and Antarctic ice sheets under 1.5°C global warming. *Nature Climate Change* 8,
1784 1053-1061.
1785

1786 Peng, P., Zhu, Y.Z., Zhong, M., Kang, K.X., Du, Z.L., Yan, H.M., 2016. Ice mass variation
1787 in Antarctica from GRACE over 2002-2011. *Marine Geodesy* 39(2), 178-194.
1788

1789 Pfeffer, W.T., Arendt, A.A., Bliss, A., Bolch, T., Cogley, J.G., Gardner, A.S., Hagen, J.O.,
1790 Hock, R., Kaser, G., Kienholz, C., Miles, E.S., Moholdt, G., Mölg, N., Paul, F., Radić, V.,
1791 Rastner, P., Raup, B.H., Rich, J., Sharp, M.J., and the Randolph Consortium, 2014. The
1792 Randolph Glacier Inventory: a globally complete inventory of glaciers. *J. Glaciol.* 60, 537–
1793 552, doi:10.3189/2014JoG13J176.
1794

1795 Pollard, D., DeConto, R.M., Alley, R.B., 2015. Potential Antarctic Ice Sheet retreat driven by
1796 hydrofracturing and ice cliff failure. *Earth Planet Sci Lett.* 412, 112–121.
1797 doi:10.1016/j.epsl.2014.12.035
1798

1799 Pollard, D., Gomez, N., DeConto, R.M., 2017. Variations of the Antarctic Ice Sheet in a
1800 coupled ice sheet-Earth-sea level model: sensitivity to viscoelastic Earth properties. *J.*
1801 *Geophys. Res.: Earth Surface* 122, 2124-2138.
1802

1803 Previdi, M., L. M. Polvani, 2016. Anthropogenic impact on Antarctic surface mass balance,
1804 currently masked by natural variability, to emerge by mid-century. *Environ. Res. Lett.* 11,
1805 094001, doi:10.1088/1748-9326/11/9/094001.
1806

1807 Radić, V., Bliss, A., Beedlow, A.C., Hock, R., Miles, E., Cogley, J.G., 2014. Regional and
1808 global projections of twenty-first century glacier mass changes in response to climate
1809 scenarios from global climate models. *Clim. Dynam.* 42, 37–58, doi:10.1007/s10712-013-
1810 9262-y.
1811

1812 Reager, J.T., Gardner, A.S., Famiglietti, J.S., Wiese, D.N., Eicker, A., Lo, M.H., 2016. A
1813 decade of sea level rise slowed by climate-driven hydrology. *Science* 351(6274), 699–703.
1814 doi:10.1126/science.aad8386.
1815

1816 Reerink, T. J., van de Berg, W. J., and van de Wal, R. S. W., 2016. OBLIMAP 2.0: a fast
1817 climate model–ice sheet model coupler including online embeddable mapping routines,
1818 *Geosci. Model Dev.* 9, 4111-4132, doi:10.5194/gmd-9-4111-2016.
1819

1820 Rietbroek, R., Brunnabend, S.E., Kusche, J., Schröter, J., Dahle, C., 2016. Revisiting the
1821 contemporary sea-level budget on global and regional scales. *Proceedings of the National*
1822 *Academy of Sciences* 113(6), 1504–1509, doi:10.1073/pnas.1519132113.
1823

1824 Rignot, E., Mouginot, J., Morlighem, M., Seroussi, H., Scheuchl, B., 2014. Widespread, rapid
1825 grounding line retreat of Pine Island, Thwaites, Smith, and Kohler glaciers, West Antarctica,
1826 from 1992 to 2011. *Geophys. Res. Lett.* 41(10), 3502-3509.
1827

1828 Rignot, E., Mouginot, J., Scheuchl, B., van den Broeke, M., van Wessem, M.J., Morlighem,
1829 M., 2019. Four decades of Antarctic Ice Sheet mass balance from 1979-2017. *PNAS* 116 (4),
1830 1095-1103.
1831

1832 Ritz, C., Edwards, T.L., Durand, G, Payne, A.J., Peyaud, V., Hindmarsh, R.C.A., 2015.
1833 Potential sea-level rise from Antarctic ice-sheet instability constrained by observations.
1834 *Nature* 528, 115-118.
1835

1836 Rodell, M., Houser, P. R., Jambor, U., Gottschalck, J., Mitchell, K., Meng, C.-J., Arsenault,
1837 K., Cosgrove, B., Radakovich, J., Bosilovich, M., Entin, J.K., Walker, J.P., Lohmann, D.,
1838 Toll, D., 2004. The Global Land Data Assimilation System. *Bull. Amer. Meteorol. Soc.* 85,
1839 381–394, doi:10.1175/BAMS-85-3-381.

1840

1841 Sasgen, I., Konrad, H., Ivins, E.R., Van den Broeke, M.R., Bamber, J.L., Martinec, Z.,
1842 Klemann, V., 2013. Antarctic ice-mass balance 2003 to 2012: regional reanalysis of GRACE
1843 satellite gravimetry measurements with improved estimate of glacial-isostatic adjustment
1844 based on GPS uplift rates. *Cryosphere*, 7(5), 1499-1512.

1845

1846 Sasgen, I., Martín-Español, A., Horvath, A., Klemann, V., Petrie, E.J., Wouters, B., Horvath,
1847 M., Pail, R., Bamber, J.L., Clarke, P.J., Konrad, H., Drinkwater, M.R., 2017. Joint inversion
1848 estimate of regional glacial isostatic adjustment in Antarctica considering a lateral varying
1849 Earth structure (ESA STSE Project REGINA). *Geophysical Journal International*, 211(3),
1850 1534-1553.

1851

1852 Sasgen, I., Konrad, H., Helm, V., Grosfeld, K., 2019. High-resolution mass trends of the
1853 Antarctic ice sheet through a spectral combination of satellite gravimetry and radar altimetry
1854 observations. *Remote Sensing* 11, 144.

1855

1856 Saunders, K.M., Roberts, S.J., Perren, B., Butz, C., Sime, L., Davies, S., Van Nieuwenhuyze,
1857 W., Grosjean, M., Hodgson, D.A., 2018. Holocene dynamics of the Southern Hemisphere
1858 westerly winds and possible links to CO₂ outgassing. *Nature Geoscience* 11 (9), 650-655.

1859

1860 Scambos, T., C. Shuman, 2016. Comment on “Mass gains of the Antarctic ice sheet exceed
1861 losses” by H.J. Zwally and others. *J. Glaciol.* 62, 599-603.

1862

1863 Schlosser, E., Stenni, B., Valt, M., Cagnati, A., Powers, J.G., Manning, K.W., Raphael, M.,
1864 Duda, M.G., 2016. Precipitation and synoptic regime in two extreme years 2009 and 2010 at
1865 Dome C, Antarctica – implications for ice core interpretation. *Atmospheric Chem. Phys.* 16,
1866 4757–4770.

1867

1868 Schoof, C., 2007. Ice sheet grounding line dynamics: steady states, stability, and hysteresis. *J.*
1869 *Geophys. Res. Earth Surf.* 112, F03S28.

1870

1871 Schrama, E.J.O., Wouters, B., Rietbroek, R., 2014. A mascon approach to assess ice sheet
1872 and glacier mass balances and their uncertainties from GRACE data. *J. Geophys. Res.: Solid*
1873 *Earth* 119, 6048–6066, doi:10.1002/2013JB010923.

1874

1875 Schroder, L., Horvath, M., Dietrich, R., Helm, V., van den Broeke, M.R., Ligtenberg,
1876 S.R.M., 2019. Four decades of Antarctic surface elevation changes from multi-mission
1877 satellite altimetry. *Cryosphere* 13, 427-449.

1878

1879 Scott, R.C., Nicolas, J.P., Bromwich, D., Norris, J.R., Lubin, D., 2019. Meteorological
1880 drivers and large-scale climate forcing of West Antarctic surface melt. *J. Clim.* 32, 665– 684.

1881

1882 Seroussi, H., Nakayama, Y., Larour, E., Menemenlis, D., Morlighem, M., Rignot, E.,
1883 Khazendar, A., 2017. Continued retreat of Thwaites Glacier, West Antarctica, controlled by
1884 bed topography and ocean circulation. *Geophys. Res. Lett.* 44, 6191–6199.

1885

1886 Seroussi, H., Nowicki, S., Simon, E., Ouchi, A. A., Albrecht, T., Brondex, J., Cornford, S.,
1887 Dumas, C., Gillet-Chaulet, F., Gladstone, R., Goelzer, H., Golledge, N., Gregory, J., Greve,
1888 R., Hoffman, M., Humbert, A., Huybrechts, P., Kleiner, T., Larour, E., Leguy, G., Lipscomb,
1889 W., Lowry, D., Mengel, M., Morlighem, M., Pattyn, F., Payne, A., Pollard, D., Price, S.,
1890 Quiquet, A., Reerink, T., Reese, R., Rodehacke, C., Schlegel, N., Shepherd, A., Sun, S.,
1891 Sutter, J., Breedam, J. V., Wal, R. v. d., Winkelmann, R., Zhang, T., 2019. initMIP-
1892 Antarctica: An ice sheet model initialization experiment of ISMIP6. *The Cryosphere* 13,
1893 1441-1471.

1894

1895 Shepherd, A., Ivins, E.R., Barletta, V.R., Bentley, M.J., Bettadpur, S., Briggs, K.H.,
1896 Bromwich, D.H., Forsberg, R., Galin, N., Horwath, M., Jacobs, S., Joughin, I., King, M.A.,
1897 Lenaerts, J.T.M., Li, J., Ligtenberg, S.R.M., Luckman, A., Luthcke, S.B., McMillan, M.,
1898 Meister, R., Milne, G., Mouginot, J., Muir, A., Nicolas, J.P., Paden, J., Payne, A.J., Pritchard,
1899 H., Rignot, E., Rott, H., Sørensen, L.S., Scambos, T.A., Scheuchl, B., Schrama, E.J.O.,
1900 Smith, B., Sundal, A.V., van Angelen, J.H., van de Berg, W.J., van den Broeke, M.R.,
1901 Vaughan, D.G., Velicogna, I., Wahr, J., Whitehouse, P.L., Wingham, D.J., Yi, D., Young, D.
1902 & Zwally, H.J., 2012. A Reconciled Estimate of Ice-Sheet Mass Balance. *Science* 338
1903 (6111), 1183-1189.

1904

1905 Shepherd, A., Ivins, E., Rignot, E., Smith, B., van den Broeke, M., Velicogna, I.,
1906 Whitehouse, P., Briggs, K., Joughin, I., Krinner, G., Nowicki, S., Payne, T., Scambos, T.,
1907 Schlegel, N., Geruo, A., Agosta, C., Ahlstrom, A., Babonis, G., Barletta, V., Blazquez, A.,
1908 Bonin, J., Csatho, B., Cullather, R., Felikson, D., Fettweis, X., Forsberg, R., Gallee, H.,
1909 Gardner, A., Gilbert, L., Groh, A., Gunter, B., Hanna, E., Harig, C., Helm, V., Horvath, A.,
1910 Horwath, M., Khan, S., Kjeldsen, K.K., Konrad, H., Langen, P., Lecavalier, B., Loomis, B.,
1911 Luthcke, S., McMillan, M., Melini, D., Mernild, S., Mohajerani, Y., Moore, P., Mouginot, J.,
1912 Moyano, G., Muir, A., Nagler, T., Nield, G., Nilsson, J., Noël, B., Ootaka, I., Pattle, M.E.,
1913 Peltier, W.R., Pie, N., Rietbroek, R., Rott, H., Sandberg-Sorensen, L., Sasgen, I., Save, H.,
1914 Scheuchl, B., Schrama, E., Schroder, L., Seo, K.W., Simonsen, S., Slater, T., Spada, G.,
1915 Sutterley, T., Talpe, M., Tarasov, L., van de Berg, W.J., van der Wal, W., van Wessem, M.,
1916 Vishwakarma, B.D., Wiese, D., Wouters, B., The IMBIE team, 2018. Mass balance of the
1917 Antarctic Ice Sheet from 1992 to 2017. *Nature* 558, 219-222.

1918

1919 Siegert, M.J., 2003. Glacial-interglacial variations in central East Antarctic ice accumulation
1920 rates. *Quaternary Science Reviews* 22, 741-750.

1921

1922 Slangen, A.B.A., van de Wal, R.S.W., 2011. An assessment of uncertainties in using volume-
1923 area modelling for computing the twenty-first century glacier contribution to sea-level
1924 change. *Cryosphere* 5, 673–686, doi:10.5194/tc-5-673-2011.

1925

1926 Slangen, A.B.A., Adloff, F., Jevrejeva, S., Leclercq, P.W., Marzeion, B., Wada, Y.,
1927 Winkelmann, R., 2017. A review of recent updates of sea level projections at global and
1928 regional scales. *Surv. Geophys.* 38(1), 385–406, doi:10.1007/s10712-016-9374-2.

1929

1930 Smeets, C.J.P.P., Kuipers Munneke, P., van As, D., van den Broeke, M.R., Boot, W.,
1931 Oerlemans, J., Snellen, H., Reijmer, C.H., van de Wal, R.S.W., 2018. The K-transect in west
1932 Greenland: Automatic weather station data (1993-2016). *Arctic, Antarctic and Alpine*
1933 *Research* 50 (1), e1420954, doi: 10.1080/15230430.2017.1420954

1934

1935 Souverijns, N., Gossart, A., Gorodetskaya, I.V., Lhermitte, S., Mangold, A., Laffineur, Q.,
1936 Delcloo, A., van Lipzig, N.P.M., 2018. How does the ice sheet surface mass balance relate to
1937 snowfall? Insights from a ground-based precipitation radar in East Antarctica. *The*
1938 *Cryosphere* 12, 1987–2003, doi:<https://doi.org/10.5194/tc-12-1987-2018>.
1939
1940 Steger, C.R., Reijmer, C.H., van den Broeke, M.R., Wever, N., Forster, R.R., Koenig, L.S.,
1941 Kuipers Munneke, P., Lehning, M., Lhermitte, S., Ligtenberg, S.R.M, Miège, C., Noël,
1942 B.P.Y., 2017. Firn meltwater retention on the Greenland ice sheet: A model comparison.
1943 *Front Earth Sci.* 5:3, doi:10.3389/feart.2017.00003.
1944
1945 Stenni, B., Scarchilli, C., Masson-Delmotte, V., Schlosser, E., Ciardini, V., Dreossi, G.,
1946 Grigioni, P., Bonazza, M., Cagnati, A., Karlicek, D., Risi, C., Udisti, R., and Valt, M., 2016.
1947 Three-year monitoring of stable isotopes of precipitation at Concordia Station, East
1948 Antarctica. *Cryosphere* 10, 2415-2428, <https://doi.org/10.5194/tc-10-2415-2016>.
1949
1950 Stewart, C.L., Christoffersen, P., Nicholls, K.W., Williams, M.J.M., Dowdeswell, J.A., 2019.
1951 Basal melting of Ross Ice Shelf from solar heat adsorption in an ice-front polynya. *Nature*
1952 *Geoscience* 12, 435-440, 10.1038/s41561-019-0356-0.
1953
1954 Stibal, M., Box, J.E., Cameron, K.A., Langen, P.L., Yallop, M.L., Mottram, R.H., Khan,
1955 A.L., Molotch, N.P., Christmas, N.A.M., Quaglia, F.C., Remias, D., Smeets, C.J.P.P., van den
1956 Broeke, M.R., Ryan, J.C., Hubbard, A., Tranter, M., van As, D., Ahlstrom, A., 2017. Algae
1957 Drive Enhanced Darkening of Bare Ice on the Greenland Ice Sheet. *Geophys Res Lett.* 44,
1958 11463-11471, doi:10.1002/2017GL075958.
1959
1960 Straneo, F., Heimbach, P., Sergienko, O., Hamilton, G., Catania, G., Griffies, S., Hallberg,
1961 R., Jenkins, A., Joughin, I., Motyka, R., Pfeffer, W.T., Price, S.F., Rignot, E., Scambos, T.,
1962 Truffer, M., Vieli, A., 2013. Challenges to Understanding the Dynamic Response of
1963 Greenland's Marine Terminating Glaciers to Oceanic and Atmospheric Forcing. *Bull. Amer.*
1964 *Meteorol. Soc.* 94, 1131-1144.
1965
1966 Sutanudjaja, E.H., van Beek, R., Wanders, N., Wada, Y., Bosmans, J.H.C., Drost, N., van der
1967 Ent, R. J., de Graaf, I.E.M., Hoch, J.M., de Jong, K., Karssenber, D., López López, P.,
1968 Peßenteiner, S., Schmitz, O., Straatsma, M.W., Vannamettee, E., Wisser, D., and Bierkens, M.
1969 F. P., 2018. PCR-GLOBWB 2: a 5 arcmin global hydrological and water resources model.
1970 *Geosci. Model Dev.*, 11, 2429-2453, <https://doi.org/10.5194/gmd-11-2429-2018>
1971
1972 Talpe, M.J., Nerem, R.S., Forootan, E., Schmidt, M., Lemoine, F.G., Enderlin, E.M.,
1973 Landerer, F.W., 2017. Ice mass change in Greenland and Antarctica between 1993 and 2013
1974 from satellite gravity measurements. *Journal of Geodesy* 91, 1283–1298.
1975
1976 Tedesco, M., Mote, T., Fettweis, X., Hanna, E., Jeyaratnam, J., Booth, J.F., Datta, R., Briggs,
1977 K., 2016. Arctic cut-off high drives the poleward shift of a new Greenland melting record.
1978 *Nature Commun.* 7: 11723.
1979
1980 Tedesco, M., Box, J.E., Cappelen, J., Fausto, R.S., Fettweis, X., Andersen, J.K., Mote, T.,
1981 Smeets, C.J.P.P., van As, D., van de Wal, R.S.W., 2018. Greenland Ice Sheet. Arctic Report
1982 Card: Update for 2018. NOAA, [https://arctic.noaa.gov/Report-Card/Report-Card-](https://arctic.noaa.gov/Report-Card/Report-Card-2018/ArtMID/7878/ArticleID/781/Greenland-Ice-Sheet)
1983 [2018/ArtMID/7878/ArticleID/781/Greenland-Ice-Sheet](https://arctic.noaa.gov/Report-Card/Report-Card-2018/ArtMID/7878/ArticleID/781/Greenland-Ice-Sheet).
1984

1985 Thomas, E.R., van Wessem, J.M., Roberts, J., Isaksson, E., Schlosser, E., Fudge, T.J.,
1986 Vallelonga, P., Medley, B., Lenaerts, J., Bertler, N., van den Broeke, M.R., Dixon, D.A.,
1987 Frezzotti, M., Stenni, B., Curran, M., Ekaykin, A.A., 2017. Regional Antarctic snow
1988 accumulation over the past 1000 years. *Clim. Past*, 13, 1491-1513, [https://doi.org/10.5194/cp-](https://doi.org/10.5194/cp-13-1491-2017)
1989 13-1491-2017.
1990
1991 Thomas R.H., Bentley, C.R., 1978. A model for Holocene retreat of the West Antarctic Ice
1992 Sheet. *Quat. Res.* 10(2), 150–170, doi:10.1016/0033-5894(78)90098-4.
1993
1994 Thompson, D.W.J., Solomon, S., Kushner, P.J., England, M.H., Grise, K.M., Karoly, D.J.,
1995 2011. Signatures of the Antarctic ozone hole in Southern Hemisphere surface climate change.
1996 *Nat. Geosci.* 4, 741–749, doi:10.1038/ngeo1296.
1997
1998 Trusel, L.D., Das, S.B., Osman, M.B., Evans, M.J., Smith, B.E., Fettweis, X., McConnell,
1999 J.R., Noël, B.P.Y., van den Broeke, M.R., 2018. Nonlinear rise in Greenland runoff in
2000 response to post-industrial Arctic warming. *Nature* 564(7734), 104-108.
2001
2002 Turner, J., J. S. Hosking, T. J. Bracegirdle, T. Phillips, G. J. Marshall, 2016. Variability and
2003 trends in the Southern Hemisphere high latitude, quasi-stationary planetary waves. *Int. J.*
2004 *Climatol.* 37, 2325–2336, doi:10.1002/joc.4848.
2005
2006 Turner, J., Phillips, T., Thamban, M., Rahaman, W., Marshall, G.J., Wille, J.D., Favier, V.,
2007 Winton, V.H.L., Thomas, E., Wang, Z., van den Broeke, M., Hosking, J.S., Lachlan-Cope,
2008 T., 2019. The dominant role of extreme precipitation events in Antarctic snowfall variability.
2009 *Geophys. Res. Lett.* 46 (6), 3502-3511, <https://doi.org/10.1029/2018GL081517>
2010
2011 Van den Broeke, M.R., Reijmer, C.H., Van de Wal, R.S.W., 2004. A study of the surface
2012 mass balance in Dronning Maud Land, Antarctica, using automatic weather station S. J.
2013 *Glaciol.* 50(171), 565-582.
2014
2015 van Den Broeke, M.R., Smeets, C.J.P.P., Van De Wal, R.S.W., 2011. The seasonal cycle and
2016 interannual variability of surface energy balance and melt in the ablation zone of the west
2017 Greenland ice sheet. *Cryosphere* 5(2), 377-390, doi:10.5194/tc-5-377-2011.
2018
2019 van Den Broeke, M.R., Enderlin, E.M., Howat, I.M., Kuipers Munneke, P., Noël, B.P.Y., van
2020 de Berg, W.J., van Meijgaard, E., Wouters, B., 2016. On the recent contribution of the
2021 Greenland ice sheet to sea level change. *Cryosphere*. 10(5). doi:10.5194/tc-10-1933-2016.
2022
2023 van den Broeke, M., Box, J., Fettweis, X., Hanna, E., Noel, B., Tedesco, M., van As, D., Van
2024 de Berg, W., van Kampenhout, L., 2017. Greenland ice sheet surface mass loss: recent
2025 developments in observation and modeling. *Curr. Clim. Change Rep.* 3, 345-356.
2026
2027 Van Kampenhout, L., Lenaerts, J.T.M., Lipscomb, W.H., Sacks, W.J., Lawrence, D.M.,
2028 Slater, A.G., van den Broeke, M.R., 2017. Improving the representation of polar snow and
2029 firn in the Community Earth System Model. *J. Adv. Model Earth Sy.* 9(7), 2583-2600.
2030
2031 Van Tricht, K., Lhermitte, S., Lenaerts, J.T.M., Gorodetskaya, I.V., L'Ecuyer, T.S., Noël, B.,
2032 van den Broeke, M.R., Turner, D.D., van Lipzig, N.P.M., 2016. Clouds enhance Greenland
2033 ice sheet meltwater runoff. *Nat Commun.* 7: 10266, doi:10.1038/ncomms10266.
2034

2035 Van Wessem, J.M., van de Berg, W.J., Noël, B.P.Y., van Meijgaard, E., Amory, C.,
2036 Birnbaum, G., Jakobs, C.L., Krüger, K., Lenaerts, J.T. M., Lhermitte, S., Ligtenberg, S.R.M.,
2037 Medley, B., Reijmer, C. H., van Tricht, K., Trusel, L.D., van Uft, L.H., Wouters, B., Wuite,
2038 J., and Van den Broeke, M.R., 2018. Modelling the climate and surface mass balance of polar
2039 ice sheets using RACMO2 – Part 2: Antarctica (1979–2016). *Cryosphere* 12, 1479-1498.
2040

2041 Van Wessem, J.M., Reijmer, C.H., Van De Berg, W.J., van den Broeke, M.R., Cook, A., van
2042 Uft, L.H., van Meijgaard, E., 2015. Temperature and wind climate of the Antarctic Peninsula
2043 as simulated by a high-resolution Regional Atmospheric Climate Model. *J Clim.* 28(18),
2044 7306-7326, doi:10.1175/JCLI-D-15-0060.1.
2045

2046 Vaughan, D.G., Comiso, J.C., Allison, I., Carrasco, J., Kaser, G., Kwok, R., Mote, P.,
2047 Murray, T., Paul, F., Ren, J., Rignot, E., Solomina, O., Steffen, K., and Zhang, T., 2013.
2048 Observations: Cryosphere, in: Stocker, T.F., Qin, D., Plattner, G.-K., Tignor, M., Allen, S.K.,
2049 Boschung, J., Nauels, A., Xia, Y., Bex, V., Midgley, P.M. (Eds.), 2013. *Climate Change*
2050 *2013: The Physical Science Basis. Contribution of Working Group I to the Fifth Assessment*
2051 *Report of the Intergovernmental Panel on Climate Change.* Cambridge University Press,
2052 Cambridge, United Kingdom and New York, NY, USA, pp. 317–382.
2053

2054 Velicogna, I., Sutterley, T.C., van den Broeke, M.R., 2014. Regional acceleration in ice mass
2055 loss from Greenland and Antarctica using GRACE time-variable gravity data. *Geophys. Res.*
2056 *Lett.* 41(22), 8130-8137.
2057

2058 Verfaillie, D., Fily, M., Le Meur, E., Magand, O., Jourdain, B., Arnaud, L., Favier, V., 2012.
2059 Snow accumulation variability derived from radar and firn core data along a 600 km transect
2060 in Adelie Land, East Antarctic plateau. *Cryosphere* 6, 1345–1358, doi:10.5194/tc-6-1345-
2061 2012.
2062

2063 Vignon, E., Genthon, C., Barral, H., Amory, C., Picard, G., Gallée, H., Casasanta, G.,
2064 Argentini, S., 2017. Momentum- and Heat-Flux Parametrization at Dome C, Antarctica: A
2065 Sensitivity Study. *Bound.-Layer Meteorol.* 162, 341–367, doi:10.1007/s10546-016-0192-3.
2066

2067 Vizcaino, M., 2014. Ice sheets as interactive components of Earth System Models: progress
2068 and challenges. *Wires Clim Change* 5(4), 557-568.
2069

2070 Vizcaino, M., Mikolajewicz, U., Groger, M., Maier-Reimer, E., Schurgers, G., Winguth,
2071 A.M.E., 2008. Long-term ice sheet-climate interactions under anthropogenic greenhouse
2072 forcing simulated with a complex Earth System Model. *Clim. Dynam.* 31(6), 665-690.
2073

2074 Vizcaino, M., Mikolajewicz, U., Jungclaus, J., Schurgers, G., 2010. Climate modification by
2075 future ice sheet changes and consequences for ice sheet mass balance. *Clim. Dynam.* 34(2-3),
2076 301-324.
2077

2078 Vizcaino, M., Lipscomb, W.H., Sacks, W.J., van den Broeke, M., 2014. Greenland Surface
2079 Mass Balance as Simulated by the Community Earth System Model. Part II: Twenty-First-
2080 Century Changes. *J. Clim.* 27(1), 215-226.
2081

2082 Vizcaino, M., Mikolajewicz, U., Ziemen, F., Rodehacke, C.B., Greve, R., van den Broeke,
2083 M.R., 2015. Coupled simulations of Greenland Ice Sheet and climate change up to A.D.
2084 2300. *Geophys. Res. Lett.* 42(10), 3927-3935.

2085
2086 Wahr, J., Wingham, D., Bentley, C., 2000. A method of combining ICESat and GRACE
2087 satellite data to constrain Antarctic mass balance. *J. Geophys. Res. Solid Earth* B7, 16279-
2088 16294.

2089 Waibel, M.S., Hulbe, C.L., Jackson, C.S. & Martin, D.F., 2018. Rate of mass loss across the
2090 instability threshold for Thwaites Glacier determines rate of mass loss for entire basin.
2091 *Geophys. Res. Lett.* 45, 809–816.
2092

2093 Weertman, J., 1974. Stability of the junction of an ice sheet and an ice shelf. *J Glaciol.*
2094 13(67), 3–11, doi:10.3198/1974JoG13-67-3-11.
2095

2096 Whitehouse, P.L., Bentley, M.J., Milne, G.A., King, M.A., Thomas, I.D., 2012. A new glacial
2097 isostatic adjustment model for Antarctica: calibrated and tested using observations of relative
2098 sea-level change and present-day uplift rates. *Geophysical Journal International*, 190(3),
2099 1464-1482.
2100

2101 Whitehouse, P.L., Gomez, N., King, M.A., Wiens, D.A., 2019. Solid Earth processes and the
2102 evolution of the Antarctic Ice Sheet. *Nature Communications* 10:503.
2103

2104 Wille, J.D., Favier, V., Dufour, A., Gorodetskaya, I.V., Turner, J., Agosta, C., Codron, F.,
2105 West Antarctic surface melt triggered by atmospheric rivers. *Nature Geoscience*, in press.
2106

2107 Williams, S.D.P., Moore, P., King, M.A., Whitehouse, P.L., 2014. Revisiting GRACE
2108 Antarctic ice mass trends and accelerations considering autocorrelation. *Earth Planet. Sci.*
2109 *Lett.* 385, 12-21.
2110

2111 Wingham, D.J., Ridout, A.L., Scharroo, R., Arthern, R.J., Shum, C.K., 1998. Antarctic
2112 elevation change 1992 to 1996. *Science* 282, 456–458.
2113

2114 Wouters, B., Bamber, J.L., van den Broeke, M.R., Lenaerts, J.T.M., Sasgen, I., 2013. Limits
2115 in detecting acceleration of ice sheet mass loss due to climate variability. *Nature Geosci.* 6(8),
2116 613-616.
2117

2118 Wouters, B., Gardner, A.S., Moholdt, G., 2019. Global glacier mass loss during the GRACE
2119 satellite mission (2002-2016). *Front. Earth Sci.*, doi.org/10.3389/feart.2019.00096.
2120

2121 Yi, D., Zwally, H.J., Cornejo, H.G., Barbieri, K.A., DiMarzio, J.P., 2011. Sensitivity of
2122 elevations observed by satellite radar altimeter over ice sheets to variations in backscatter
2123 power and derived corrections. *CryoSat Validation Workshop*, 1–3 February 2011, Frascati,
2124 Italy. European Space Research Institute, European Space Agency, Frascati, ESA SP-693
2125

2126 Yi, S., Sun, W., Heki, K., Qian, A., 2015. An increase in the rate of global mean sea level
2127 since 2010. *Geophys. Res. Lett.* 42, 3998–4006, doi:10.1002/2015GL063902.
2128

2129 Zammit-Mangion, A., Rougier, J., Schon, N., Lindgren, F., Bamber, J., 2015. Multivariate
2130 spatio-temporal modelling for assessing Antarctica's present-day contribution to sea-level
2131 rise. *Environmetrics* 26(3), 159-177.
2132

2133 Zekollari, H., Huss, M., Farinotti, D., 2019. Modelling the future evolution of glaciers in the
2134 European Alps under the EURO-CORDEX RCM ensemble. *Cryosphere* 13, 1125–1146,
2135 doi:10.5194/tc-13-1125-2019.
2136
2137 Zemp, M., Frey H., Gärtner-Roer, I., Nussbaumer, S.U., Hoelzle, M., Paul, F., Haeberli, W.,
2138 Denzinger, F., Ahlstrøm, A.P., Anderson, B., Bajracharya, S., Baroni, C., Braun, L.N.,
2139 Cáceres, B.E., Casassa, G., Cobos, G., Dávila, L.R., Delgado Granados, H., Demuth, M.N.,
2140 Espizua, L., Fischer, A., Fujita, K., Gadek, B., Ghazanfar, A., Hagen, J.O., Holmlund, P.,
2141 Karimi, N., Li, Z., Pelto, M., Pitte, P., Popovnin, V.V., Portocarrero, C.A., Prinz, R.,
2142 Sangewar, C.V., Severskiy, I., Sigurdsson, O., Soruco, A., Usabaliev, R., Vincent, C., 2015.
2143 Historically unprecedented global glacier decline in the early 21st century. *J. Glaciol.* 61,
2144 228, 745–762, doi:10.3189/2015JoG15J017.
2145
2146 Zemp, M., Huss, M., Thibert, E., Eckert, N., McNabb, R., Huber, J., Barandun, M.,
2147 Machguth, H., Nussbaumer, S.U., Gärtner-Roer, I., Thomson, L., Paul, F., Maussion, F.,
2148 Kutuzov, S., Cogley, J.G., 2019. Global glacier mass changes and their contributions to sea-
2149 level rise from 1961 to 2016. *Nature* 568, 382–386, doi:10.1038/s41586-019-1071-0.
2150
2151 Zhang, B., Liu, L., Khan, S.A., van Dam, T., Bjørk, A.A., Peings, Y., Zhang, E., Bevis, M.,
2152 Yao, Y., Noël, B., 2019. Geodetic and model data reveal different spatio-temporal patterns of
2153 transient mass changes over Greenland from 2007 to 2017. *Earth Planet. Sci. Lett.* 515, 154-
2154 163.
2155
2156 Zhang, B.J., Wang, Z.M., Li, F., An, J.C., Yang, Y.D., Liu, J.B., 2017. Estimation of present-
2157 day glacial isostatic adjustment, ice mass change and elastic vertical crustal deformation over
2158 the Antarctic ice sheet. *J. Glaciol.* 63(240), 703-715.
2159
2160 Zwally, H.J., M.B. Giovinetto, J. Li, H.G. Cornejo, M.A. Beckley, A.C. Brenner, J.L. Saba,
2161 D. Yi, 2005. Mass changes of the Greenland and Antarctic ice sheets and shelves and
2162 contributions to sea-level rise: 1992–2002. *J. Glaciol.* 51, 509–527, doi: 10.3189/
2163 172756505781829007.
2164
2165 Zwally, H.J., Li, J., Robbins, J.W., Saba, J.L., Yi, D., Brenner, A.C., 2015. Mass gains of the
2166 Antarctic ice sheet exceed losses. *J. Glaciol.* 61, 1019-1036.
2167
2168 Zwally, H.J., J. Li, J.W. Robbins. J.L. Saba, D. Yi, A.C. Brenner, 2016. Response to
2169 Comment by T. Scambos and C. Shuman (2016) on ‘Mass gains of the Antarctic ice sheet
2170 exceed losses’ by H. J. Zwally and others (2015). *J. Glaciol.*, available on CJO 2016
2171 doi:10.1017/jog.2016.91.
2172
2173
2174
2175
2176
2177
2178
2179
2180
2181
2182

2183 **Table 1.** Probabilistic projections (5th, 25th, 50th, 75th and 95th percentiles) of Antarctic
 2184 sea-level contribution at 2300 (in metres) under RCP8.5. Colour legend: **L14**: Simulations by
 2185 Levermann et al. (2014), **G15**: Simulations by Golledge et al. (2015), **DP16**: Simulations by
 2186 DeConto and Pollard (2016), **DP16BC**: Bias-corrected simulations by DeConto and Pollard
 2187 (2016), **B19S**: Simulations with Schoof’s parameterisation by Bulthuis et al. (2019), **B19T**:
 2188 Simulations with Tsai’s parameterisation by Bulthuis et al. (2019), **E19MICI**: Simulations
 2189 with MICI by Edwards et al. (2019).
 2190

	5%	25%	50%	75%	95%
L14	0.30	0.64	1.06	1.75	3.54
G15	1.61	2.07	2.28	2.50	2.96
DP16	6.86	7.35	9.05	11.09	11.25
DP16BC	6.94	7.37	9.05	11.08	11.27
B19S	0.27	0.61	1.04	1.47	1.81
B19T	0.59	1.16	1.85	2.55	3.12
E19MICI	7.08	8.28	8.90	9.51	10.71

2191
 2192
 2193
 2194
 2195
 2196
 2197
 2198
 2199
 2200
 2201
 2202
 2203
 2204
 2205
 2206
 2207
 2208
 2209
 2210
 2211
 2212
 2213
 2214
 2215
 2216
 2217

2218 **Table 2.** Pentad mass balance rates for all glaciers and ice caps, excluding the peripheral
 2219 glaciers of Greenland and Antarctica. Modified from Bamber et al. (2018). The contributions
 2220 from the peripheral glaciers are here excluded because in Bamber et al. (2018) the peripheral
 2221 glacier contributions are included in those of the corresponding ice sheet because most data
 2222 sources (many of them from GRACE) do not separate the peripheral glacier contributions.
 2223 For reference, the mass-change rates during 2003-2009, according to Gardner et al. (2013),
 2224 were of -38 ± 7 Gt yr⁻¹ (0.10 ± 0.02 mm SLE yr⁻¹) for the Greenland peripheral glaciers, and of
 2225 -6 ± 10 Gt yr⁻¹ (0.02 ± 0.03 mm SLE yr⁻¹) for the Antarctic peripheral glaciers. According to
 2226 Zemp et al. (2019), the contributions during 2002-2016 were of -51 ± 17 Gt yr⁻¹ (0.14 ± 0.05
 2227 mm SLE yr⁻¹) for Greenland periphery and -14 ± 108 Gt yr⁻¹ (0.00 ± 0.30 mm SLE yr⁻¹) for the
 2228 Antarctic periphery.
 2229

Pentad	1992-1996	1997-2001	2002-2006	2007-2011	2012-2016
Gt yr ⁻¹	-117 ± 44	-149 ± 44	-173 ± 33	-197 ± 30	-227 ± 31
mm SLE yr ⁻¹	0.32 ± 0.12	0.42 ± 0.12	0.48 ± 0.09	0.55 ± 0.08	0.63 ± 0.08

2230
 2231
 2232
 2233
 2234
 2235
 2236
 2237
 2238
 2239
 2240
 2241
 2242
 2243
 2244
 2245
 2246
 2247
 2248
 2249
 2250
 2251
 2252
 2253
 2254
 2255
 2256
 2257
 2258
 2259
 2260
 2261
 2262
 2263

2264 **Table 3.** Estimated contributions to sea-level rise by glaciers and by ice sheets over different
 2265 recent periods. The data sources are indicated. The percentages indicate the relative
 2266 contributions of the glaciers and of the ice sheets with respect to the total contribution from
 2267 the landed ice masses.
 2268

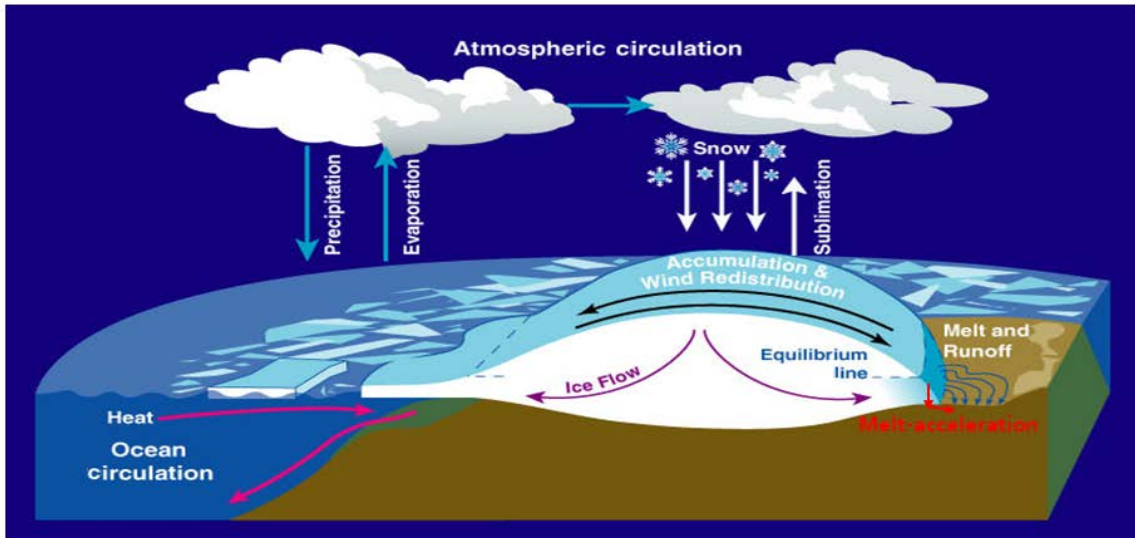
	1993-2010 Church et al. (2013) (IPCC AR5)		2003/05-2009/10 Gardner et al. (2013) Shepherd et al. (2012)		2012-2016 modified from Bamber et al. (2018)	
	mm SLE yr ⁻¹	%	mm SLE yr ⁻¹	%	mm SLE yr ⁻¹	%
Glaciers	0.86	59	0.72	43	0.73 ^a	40 ^{a,b}
Ice sheets	0.60	41	0.95	57	1.10 ^{a,b}	60 ^{a,b}

2269
 2270 ^a Including the contributions from the peripheral glaciers of Greenland and Antarctica.
 2271 ^b If the more recent estimate for the Antarctic Ice Sheet by Shepherd et al. (2018) for 2012-
 2272 2017 were taken instead of that by Bamber et al. (2018) for 2012-2016, the contribution from
 2273 the ice sheets would increase to 1.29 mm SLE yr⁻¹ and the relative contributions would be of
 2274 36% for glaciers and 64% for ice sheets.
 2275
 2276
 2277
 2278
 2279
 2280
 2281
 2282
 2283
 2284
 2285
 2286
 2287
 2288
 2289
 2290
 2291
 2292
 2293
 2294
 2295
 2296
 2297
 2298
 2299
 2300
 2301
 2302
 2303
 2304
 2305
 2306
 2307

2308 **Figures**

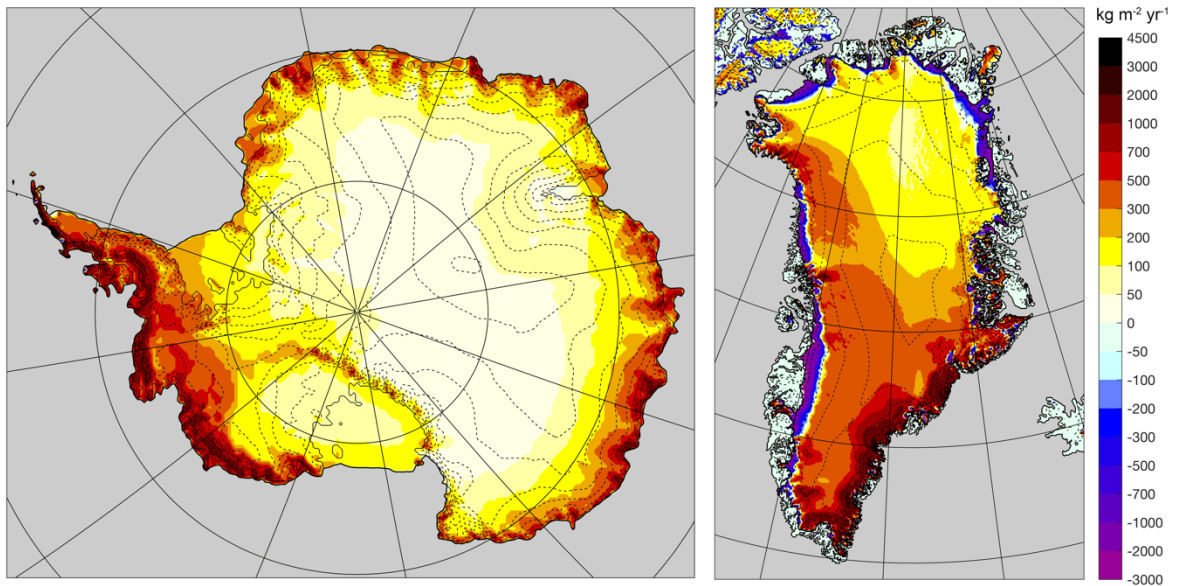
2309

2310 **Figure 1.** The main processes affecting the mass balance and dynamics of ice sheets. Mass
2311 input from snowfall is balanced by losses from surface meltwater runoff, sublimation and
2312 dynamical mass losses (solid ice discharge across the grounding line). Surface melting is
2313 highly significant for Greenland but for Antarctic grounded ice is very small and subject to
2314 refreezing. Interaction with the ocean occurs at the undersides of the floating ice shelves and
2315 glacier tongues, and consequent changes in thickness affect the rate of ice flow from the
2316 grounded ice. Reproduced from Zwally et al. (2015) with the permission of Jay Zwally.



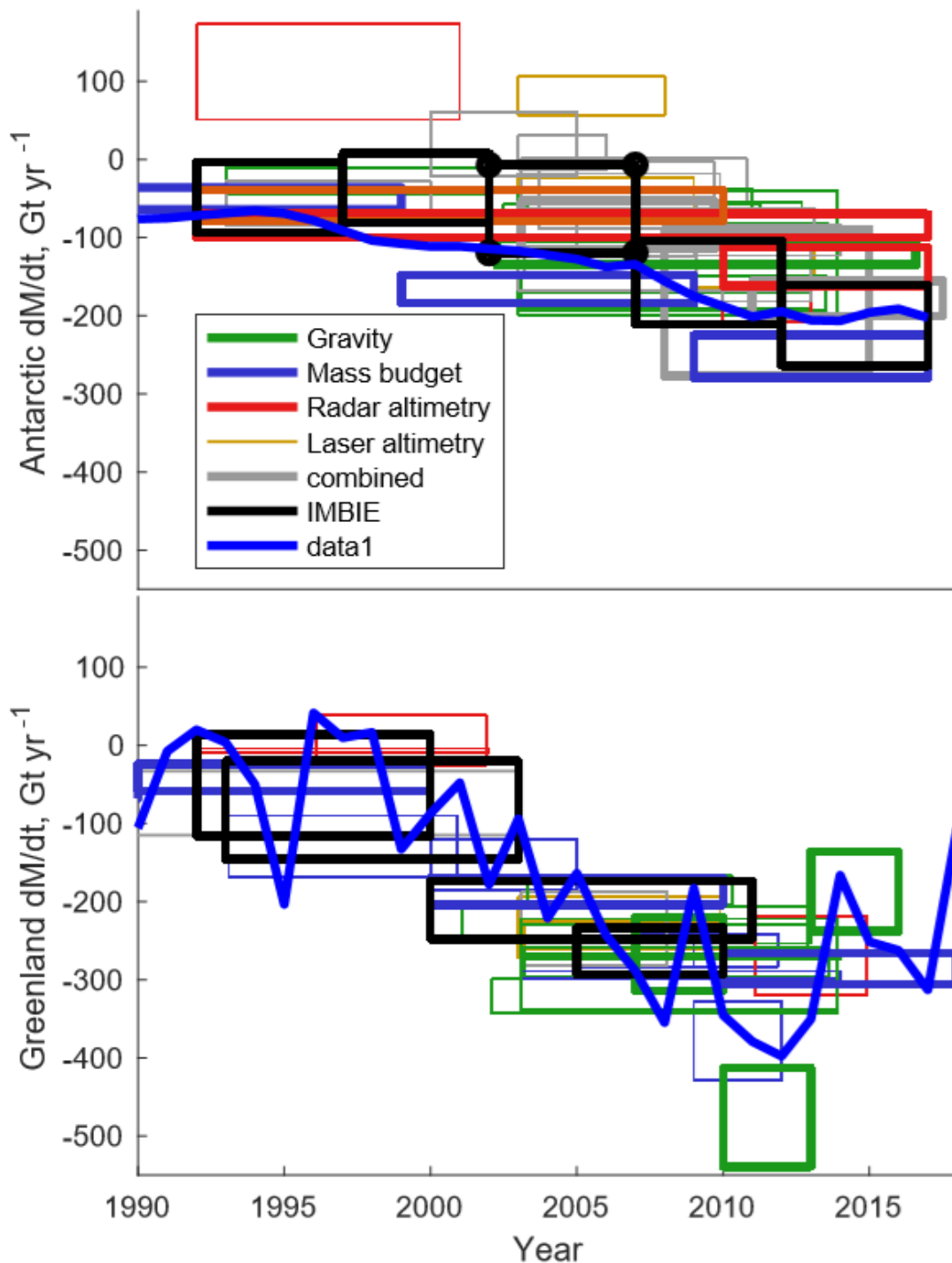
2317
2318
2319
2320
2321
2322
2323
2324
2325
2326
2327
2328
2329
2330
2331
2332
2333
2334

2335 **Figure 2.** Surface mass balance (averaged over the period 1989-2009) of the Antarctic ice
2336 sheets (left) and the Greenland Ice Sheet (right) from the regional climate model
2337 RACMO2.3p2 in $\text{kg m}^{-2} \text{yr}^{-1}$ (van Wessem et al., 2018; Noël et al., 2018a). Elevation contour
2338 levels (dashed) are shown every 500 m.



2339
2340
2341
2342
2343
2344
2345
2346
2347
2348
2349
2350
2351
2352
2353
2354
2355
2356
2357
2358
2359
2360
2361
2362
2363
2364
2365
2366
2367
2368

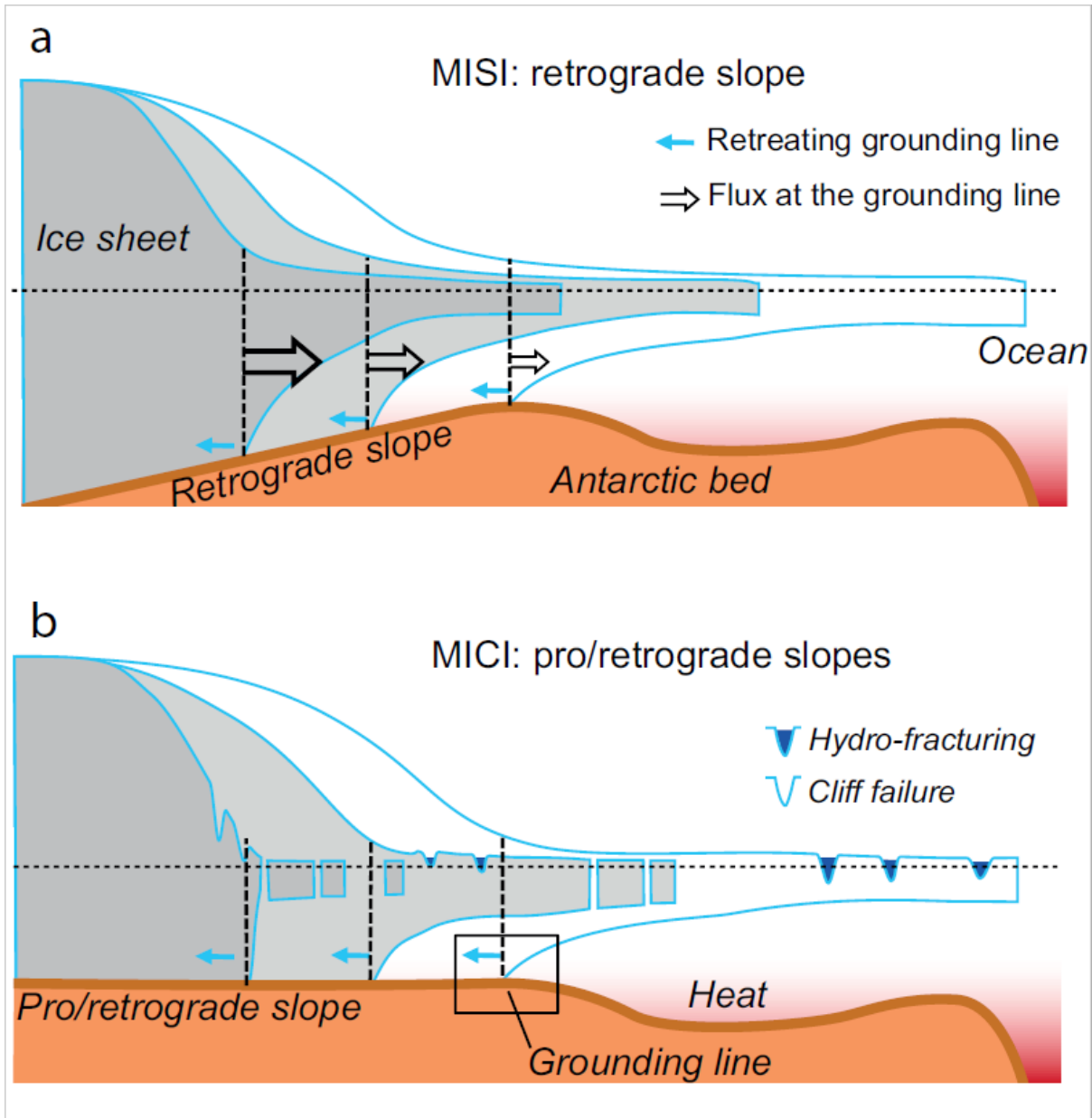
2369 **Figure 3.** Mass rates for the Antarctic (top) and Greenland (bottom) ice sheets derived from
 2370 published studies. The horizontal extent of each rectangle indicates the period that each
 2371 estimate spans, while the height indicates the error estimate. Studies published between 2011
 2372 and 2017 are shown with thin lines, studies published in 2018 and early 2019 with heavier
 2373 lines. The colour of the lines indicates the type of estimate used, and any estimate that is
 2374 based explicitly on more than one technique is treated as a ‘combined’ estimate. The
 2375 IMBIE (Shepherd et. al, 2012 for Greenland, Shepherd et al., 2018 for Antarctica) estimates
 2376 are shown in black. Rectangles are overplotted with annual mass balance estimates from
 2377 Rignot et al. (2019) for Antarctica and Mouginot et al. (2019) for Greenland, to indicate
 2378 interannual variability. The studies cited in this plot are described in Supplemental Table I.
 2379



2380

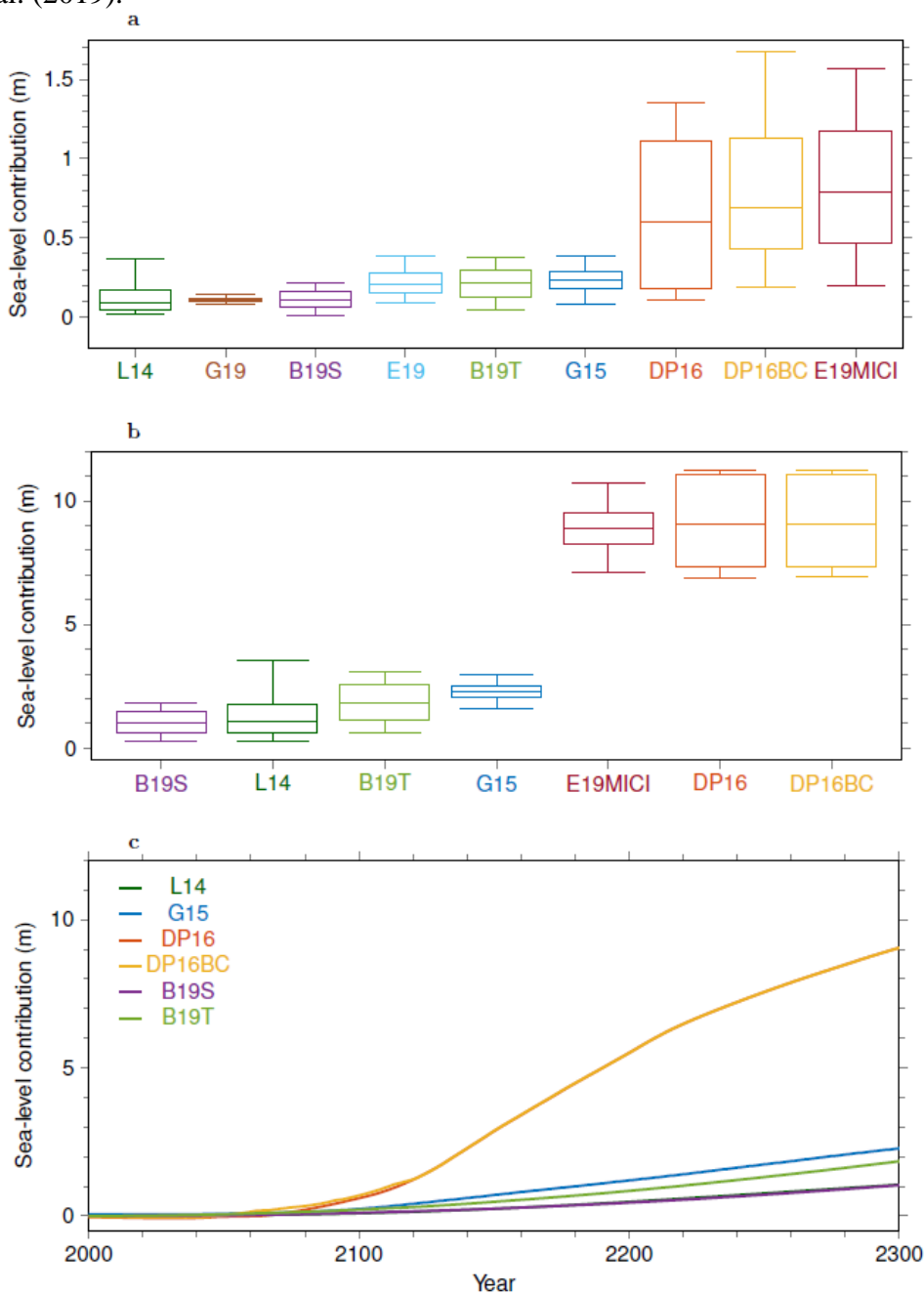
2381
2382
2383

Figure 4. Schematics of (a) Marine Ice Shelf Instability (MISI) and (b) Marine Ice Cliff Instability (MICI). The reader is referred to Section 3.1 for a discussion of MISI/MICI.



2384
2385
2386
2387
2388
2389
2390
2391
2392
2393
2394
2395
2396
2397
2398

2399 **Figure 5.** Projections of Antarctic sea-level contribution at (a) 2100 and (b) 2300 under
 2400 RCP8.5. Boxes and whiskers show the 5th, 25th, 50th, 75th and 95th percentiles. The
 2401 uncertainty range for Golledge et al. (2015) is based on a Gaussian interpretation for the
 2402 projections with the 5th percentile given by the low scenario and the 95th percentile given by
 2403 the high scenario. Idem for Golledge et al. (2019) with the 5th percentile given by the
 2404 simulation without melt feedback and the 95th percentile given by the simulation with melt
 2405 feedback. (c) Median projections of Antarctic sea-level contribution until 2300 (RCP8.5).
 2406 Colour legend: **L14**: Simulations by Levermann et al. (2014), **G15**: Simulations by Golledge
 2407 et al. (2015), **DP16**: Simulations by DeConto and Pollard (2016), **DP16BC**: Bias-corrected
 2408 simulations by DeConto and Pollard (2016), **B19S**: Simulations with Schoof's
 2409 parameterisation by Bulthuis et al. (2019), **B19T**: Simulations with Tsai's parameterisation
 2410 by Bulthuis et al. (2019), **E19**: Simulations without MICI by Edwards et al. (2019),
 2411 **E19MICI**: Simulations with MICI by Edwards et al. (2019), **G19**: Simulations by Golledge
 2412 et al. (2019).



2413

Supplementary Information

Supplemental table I. Details of mass-balance estimates used in Figure 4. Key for measurement type: G = gravimetry, L = laser altimetry, IOM = in/out (mass budget) method, A = airborne photogrammetry, RL and GLRIOM = combined.

(a) Greenland Ice Sheet

Reference	Year	Type	Time 0	Time 1	Rate	Error
Zwally et al. 2011	2011	R	1992	2002	-7	3
Zwally et al. 2011	2011	L	2003.6	2007.8	-171	4
Shepherd et al. 2012	2012	GLRIOM	1992	2000	-51	65
“	2012	GLRIOM	1993	2003	-83	63
“	2012	GLRIOM	2000	2011	-211	37
“	2012	GLRIOM	2005	2010	-263	30
Wouters et al. 2013	2013	G	2003.1	2012.9	-249	20
Csatho et al. 2014	2014	L	2003.2	2010	-243	18
Enderlin et al. 2014	2014	IOM	2000	2005	-153	33
“	2014	IOM	2005	2009	-265	18
“	2014	IOM	2009	2012	-378	50
Groh et al. 2014	2014	L	2003	2009.9	-233	39
“	2014	G	2001.1	2013	-230	23.5
Hurkmans et al. 2014	2014	R	1996.1	2001.9	6	32.1
“	2014	RL	2003.1	2008.1	-235	47
Schrama et al. 2014	2014	G	2003.2	2013.6	-278	19
Velicogna et al. 2014	2014	G	2003.1	2013.9	-280	58
Andersen et al. 2015	2015	IOM	2007.1	2011.9	-262	21
Kjeldsen et al. 2015	2015	A	1983	2003	-74	41
“	2015	G	2003.3	2010.3	-186	18.9
McMillan et al. 2016	2016	R	2011.1	2014.9	-269	51
van den Broeke et al. 2016	2016	G	2003.1	2014	-270	4
“	2016	IOM	2003.1	2014	-294	5

Talpe et al. 2017	2017	G	2002.1	2013.9	-321	22
“	2017	IOM	1993.1	2000.9	-129	39
Mouginot et al. 2019	2019	IOM	1990	2000	-41.1	17
“	2019	IOM	2000	2010	-186.7	17
“	2019	IOM	2010	2018	-286.2	20
Zhang et al. 2019	2019	G	2007	2010	-267	47
“	2019	G	2010	2013	-476	63
“	2019	G	2013	2016	-187	51

(b) Antarctic ice sheets

Reference	Year	Type	Time 0	Time 1	Rate	Error
King et al. 2012	2012	G	2002.7	2010.9	-78	49
Bauer et al. 2013	2013	G	2002.5	2011.4	-104	48
Ivins et al. 2013	2013	G	2003	2012	-57	34
Sasgen et al. 2013	2013	G	2003	2012.7	-114	23
Groh et al. 2014b	2014	L	2003.1	2009.1	-126	39
Groh et al. 2014b	2014	G	2003.1	2009.1	-95	24
Gunter et al. 2014	2014	LG	2003.2	2009.1	-100	44
McMillan et al. 2014	2014	R	2010	2013	-159	48
Memin et al. 2014	2014	GR	2003.1	2010.8	-28	29
Schrama et al. 2014	2014	G	2003.1	2013.5	-171	22
Velicogna et al. 2014	2014	G	2003	2013	-180	10
Williams et al. 2014	2014	G	2003.3	2012.7	-62	7
Gao et al. 2015	2015	G	2003	2013.9	-120	80
Harig and Simons 2015	2015	G	2003.2	2013.6	-92	10
Li et al. 2016	2016	L	2003	2009	-44	21
Zamit-Magion et al. 2015	2015	LRG	2003	2009.9	-47	29
Zwally et al. 2015	2015	L	2003	2008	82	25
Zwally et al. 2015	2015	R	1992	2001	112	61
Jin et al. 2016	2016	G	1993	2002	-28	17

Jin et al. 2016	2016	G	2003	2011	-55	17
Martín-Español et al. 2016	2016	LRG	2003	2013.12	-84	22
Martín-Español et al. 2016	2016	LRG	2003	2006	9	22
Martín-Español et al. 2016	2016	LRG	2007	2009	-104	21
Martín-Español et al. 2016	2016	LRG	2010	2013	-159	22
Peng et al. 2016	2016	G	2002.5	2011.25	-65	7
Sasgen et al. 2017	2017	RG	2003	2013	-141	27
Shepherd et al. 2018	2018	LRG/IO	1992	1997	-48	45
Shepherd et al. 2018	2018	R/IO	1997	2002	-37	44
Shepherd et al. 2018	2018	LRG/IO	2002	2007	-63	56
Shepherd et al. 2018	2018	LRG/IO	2007	2012	-158	53
Shepherd et al. 2018	2018	RG/IO	2012	2017	-213	51
Talpe et al. 2017	2017	G/IO	1993	2000	-56	28
Talpe et al. 2017	2017	G/IO	2000	2005	20	41
Talpe et al. 2017	2017	G/IO	2005	2014	-103	20
Zhang et al. 2017	2017	LGG	2003.7	2009.7	-46	43
Gardner et al. 2018	2018	IO	2008	2015	-183	94
Gao et al. 2019a	2019	G	2002.25	2016.6	-119	16
Gao et al. 2019b	2019	LRG	2003.1	2009.7	-84	31
Rignot et al. 2019	2019	IOM	1979	1989	-40	9
Rignot et al. 2019	2019	IOM	1989	1999	-50	14
Rignot et al. 2019	2019	IOM	1999	2009	-166	18
Rignot et al. 2019	2019	IOM	2009	2017	-252	27
Sasgen et al. 2019	2019	RG	2011	2017.5	-178	23
Schroder et al. 2019	2019	R	1992	2017	-85	15
Schroder et al. 2019	2019	LR	1992	2010	-59	20
Schroder et al. 2019	2019	R	2010	2017	-137	25

